Chem Soc Rev

REVIEW ARTICLE

View Article Online
View Journal | View Issue

Check for updates

Cite this: *Chem. Soc. Rev.*, 2025, **54**, 1583

Molecular insights into the composition, sources, and aging of atmospheric brown carbon

Alexander Laskin, *[ab] Christopher P. West [a] and Anusha P. S. Hettiyadura [a]

The light-absorbing chemical components of atmospheric organic aerosols are commonly referred to as Brown Carbon (BrC), reflecting the characteristic yellowish to brown appearance of aerosol. BrC is a highly complex mixture of organic compounds with diverse compositions and variable optical properties of its individual chromophores. BrC significantly influences the radiative budget of the climate and contributes to adverse air pollution effects such as reduced visibility and the presence of inhalable pollutants and irritants. However, a fundamental understanding of the sources, formation, and transformation (aging effects) of BrC remains incomplete. This gap in knowledge necessitates advanced chemical characterization of individual aerosol components and the correlation of their composition with optical properties. Over the past decade, a multi-modal analytical platform composed of high-performance liquid chromatography with a photodiode array UV-vis detector and high-resolution mass spectrometry has been extensively used for the untargeted analysis of BrC components in complex mixtures of atmospheric organic aerosols and their laboratory proxies. This method separates solvent-extractable BrC compounds into distinct fractions, each characterized by specific retention times, UV-vis absorption spectra, and elemental compositions, offering comprehensive molecular insights into BrC components. In this review, we highlight the application of this platform in analyzing both real-world aerosol samples and laboratory-generated proxies. These studies have identified composition-specific sources and transformations of BrC, advancing our understanding of these complex atmospheric mixtures. Atmospheric humic-like substances (HULIS), formed through cloud processing of wildfire smoke and the oligomerization of water-soluble organics, are key contributors to BrC. Additional HULIS originate from fossil fuel combustion, biogenic, and marine emissions. Key BrC chromophores include nitroaromatics, imidazoles, N-heterocycles, polyaromatic hydrocarbons, quinones, and others. Aging processes, including photolysis and multiphase reactions, can significantly alter BrC optical properties by generating new chromophores or degrading existing ones. The fundamental knowledge gained from these investigations is essential for assessing BrC optical properties. Additionally, it provides practical composition metrics necessary to inform and improve future atmospheric models, enabling more accurate predictions of BrC behavior and its impact on climate and air quality.

Received 23rd August 2023

DOI: 10.1039/d3cs00609c

rsc.li/chem-soc-rev

Open Access Article. Published on 02 January 2025. Downloaded on 1/23/2026 11:08:06 PM.
This article is licensed under a Creative Commons Attribution-NonCommercial 3.0 Unported Licence.

1. Introduction

Atmospheric Brown Carbon (BrC)[1] is a complex mixture of light-absorbing components present in organic aerosol (OA), exhibiting diverse compositions[2] and variable optical properties.[3] Ambient BrC typically exhibits featureless UV-vis spectra, with absorption that intensifies at shorter, UV wavelengths. The environmental effects of BrC range from local visibility reduction to climate forcing, resulting from its direct interactions with solar and terrestrial radiation, and its indirect effects on cloud formation and microphysics. In many regions,[4–13] the overall impact of BrC rivals or even exceeds that of more commonly considered atmospheric aerosol light absorbers such as black carbon (BC) and mineral dust (MD). However, the quantitative assessment of BrC's direct radiative effects by climate models remains highly uncertain, with estimates[14–22] ranging from +0.03 W m^{-2} to +0.57 W m^{-2}. This uncertainty is intrinsically related to the variability and complexity of BrC sources, composition, chemical aging, and absorption properties. Only in the past decade quantitative descriptions of BrC's composition and properties have begun to emerge, driven by molecular characterization studies linking its composition and optical properties to emission sources.

Primary BrC emissions, resulting mostly from the incomplete combustion of biomass, hold significant atmospheric importance.[1]

[a] *Department of Chemistry, Purdue University, West Lafayette, Indiana, 47906, USA. E-mail: alaskin@purdue.edu*
[b] *Department of Earth, Atmospheric & Planetary Sciences, Purdue University, West Lafayette, Indiana, 47906, USA*

Open Access Article. Published on 02 January 2025. Downloaded on 1/23/2026 11:08:06 PM. This article is licensed under a Creative Commons Attribution-NonCommercial 3.0 Unported Licence.

Such emissions are prevalent in areas experiencing biomass burning, including forest wildfires, intentional deforestation, prescribed burns for forest management, agricultural fires, and regions where wood and other biofuels are extensively used for heating, cooking, and energy production. In urban areas, significant amounts of primary BrC are emitted from fossil fuel combustion, primarily stemming from vehicle exhaust[23–26] and use of coal for heating and power generation.[25–28] Additionally, secondary organic aerosols (SOA) formed from the oxidation of volatile organic compounds (VOCs) from various sources (both related and unrelated to biomass burning) contribute to secondary BrC through multiphase gas-particle reactions.[29–40] Further condensed phase reactions in aerosol particles and cloud micro-droplets also produce secondary BrC chromophores. The distinction between primary and secondary BrC often becomes blurred due to atmospheric aging through multi-phase chemical reactions and particle microphysical processes, resulting in atmospheric BrC containing mixed chromophores from various origins. The various aspects of atmospheric BrC research were first reviewed by Andreae and Gelencser (2006),[1] and have since been further explored in subsequent reviews by Laskin *et al.* (2015),[2] Yan *et al.* (2018),[41] Y. Wang *et al.* (2020),[42] Hems *et al.* (2021).[43] and Q. Wang *et al.* (2023).[44] These reviews summarized significant experimental observations and modeling studies that distinguish BrC from other organic aerosol types and reported on their atmospheric presence and transformations.

Emerging conceptual understanding of the relationship between BrC's optical properties and its molecular chromophores has provided essential experimental input for a recently proposed optical-based classification of BrC.[45] Based on substantial differences in optical properties, four major BrC classes have been defined: Very Weakly (VW) absorbing BrC – formed in the photochemical processes of anthropogenic SOA formation and its aging chemistry.[46–56] Weakly (W) and Moderately (M) absorbing BrC – primarily attributed to biomass burning emissions,[30,33,38,57–66] with specific optical properties heavily influenced by the composition and moisture content of biomass fuels and variations in burning conditions. Strongly (S) absorbing BrC – attributed to highly viscous, glassy carbonaceous particles such as atmospheric tar balls[67–69] and soil organic matter.[70] Chemical studies of BrC representative of each of these classes reveal a diverse array of physicochemical traits, including molecular size, elemental and structural composition, oxidation state, volatility, glass transition

Alexander Laskin

Dr Alexander Laskin is a Professor of Chemistry at Purdue University. He completed his undergraduate degree in Physics at the Polytechnical Institute, St. Petersburg, Russia, in 1991, and earned his PhD in Physical Chemistry from the Hebrew University of Jerusalem, Israel, in 1998. Following postdoctoral appointments, he served as a staff scientist at the Pacific Northwest National Laboratory (PNNL) from 2001 to 2017. His research interests span the physical and analytical chemistry of aerosols, their environmental and atmospheric impacts, the molecular-level analysis of complex environmental mixtures and chemical imaging of individual particles. His work has produced over 250 publications, including lead and contributing authorship on peer-reviewed papers, invited reviews, and book chapters. These contributions have significantly advanced our understanding of aerosols and their wide-ranging environmental impacts.

Christopher P. West

Dr Christopher P. West earned his undergraduate degree in Chemistry from Methodist University in Fayetteville, NC, in 2016 and his PhD in Analytical Chemistry from Purdue University in 2022. During his PhD studies, he conducted fundamental research aimed at understanding the fate and reactivity of organic and mixed organic–inorganic aerosols from combustion and biogenic sources. His work included developing and integrating novel separation techniques and high-resolution mass spectrometry methods to characterize the molecular composition of complex aerosol mixtures. Currently, he is employed at Northrop Grumman as an RF Systems Engineer, where he specializes in electronic countermeasures, RF subsystem design, and system characterization.

Anusha P. S. Hettiyadura

Dr Anusha Hettiyadura earned her undergraduate degree in Chemistry from the University of Kelaniya, Sri Lanka, in 2011 and her PhD in Analytical Chemistry from the University of Iowa in 2018. She subsequently worked as a postdoctoral research associate in Dr A. Laskin's group at Purdue University from 2018 to 2021. An expert in LC-MS method development, analytical chemistry, and atmospheric chemistry, her research has been instrumental in advancing the molecular characterization of atmospheric brown carbon. She currently serves as an LC-MS Method Development Scientist at Labcorp Bioanalytical Services LLC.

This journal is © The Royal Society of Chemistry 2025

Open Access Article. Published on 02 January 2025. Downloaded on 1/23/2026 11:08:06 PM.
This article is licensed under a Creative Commons Attribution-NonCommercial 3.0 Unported Licence.

temperature, and aqueous solubility.[2,3,45,71–74] These characteristics provide valuable parameters for assessing and classifying real-world BrC across these classes. However, practical parameterization approaches hinge on an improved understanding of the relationship between BrC's molecular composition and its light-absorption properties. Existing evidence indicates that even trace amounts of strongly absorbing chromophores can dominate the optical behavior oof bulk BrC. Therefore, unraveling these relationships requires advanced analytical techniques capable of isolating, detecting, and characterizing individual BrC chromophores. A combined analytical platform of high-performance liquid chromatography (HPLC), photodiode array (PDA) detector, and high-resolution mass spectrometry (HRMS) has emerged as a preferred method for the chemical characterization of BrC components of complex environmental mixtures.[33,38,58–60,75–79] This technique separates solvent-extractable BrC compounds into fractions with characteristic retention times, UV-vis absorption spectra, and elemental compositions, offering a detailed molecular characterization of potential chromophores.[80,81]

Identifying BrC components is essential for understanding the relationship between chemical composition and optical properties. Commonly identified chromophores include nitroaromatics, methoxyphenols, imidazoles along with other N-heterocyclics, polycyclic aromatic hydrocarbons, quinones, oligomeric dihydrofurans, and various other compounds.[2,78,82] However, BrC characterization remains notoriously challenging due to the low abundance, high variability of light-absorbing molecules, and the disproportionate influence of minor but highly potent chromophores. These BrC chromophores typically constitute less than 2% of OA mass but contribute 25–30% of its light absorption.[83–86] Despite significant progress in experimental studies, the variability of BrC composition and optical properties remains only partially explained by identified chromophores, limiting the accuracy of predictive models. Recently, advanced machine learning approaches have shown great promise in inferring the properties of unidentified chromophores,[87–93] thereby improving our understanding of the relationship between BrC composition and optical behavior and paving the way for future advancements. The molecular identification of BrC chromophores offers crucial insights into emission source contributions, enabling differentiation between biomass burning, fossil fuel combustion, urban anthropogenic, and other origins. These source-specific characterizations of BrC composition and light absorption, combined with a predictive understanding of their aging transformations, have facilitated the integration of BrC into regional coupled meteorology-chemistry models.[94–97] These recent advancements enable the quantification of BrC's atmospheric concentrations and absorption effects on radiative forcing, regional weather patterns, and air quality, providing valuable insights for specific regions and timeframes.

This review presents a comprehensive summary of the current understanding regarding the molecular composition and optical properties of BrC chromophores, based on novel HPLC–PDA–HRMS experimental studies. Following the Introduction, Section 2 provides a concise overview of the analytical chemistry aspects and offers recommendations relevant to the collection, preparation, chromatography separation, and mass spectrometry detection of BrC constituents. Section 3 explores measurements and observations of BrC species in real-world samples, including aerosols, cloud and fog water, biomass burning smoke generated in controlled test facilities, and organic pollutant deposits in snowpack. This section also summarizes observations from laboratory ageing experiments conducted with field collected BrC to simulate plausible atmospheric transformations. Section 4 presents a systematic account of chemically distinct types of BrC, identified through focused laboratory studies with various organic aerosol proxies, and discusses the formation and ageing of secondary BrC chromophores. Section 5 highlights recent advancements in integrating the molecular composition of BrC into modeling frameworks. It showcases the application of machine learning to predict optical properties based on composition data. It also discusses how new insights into BrC composition and transformations improve modeling of its regional variability and impacts. Finally, Section 6 presents the authors' perspectives on existing knowledge gaps, future research directions, and anticipated experimental and data analysis developments in the field.

2. Analytical aspects of BrC chemical characterization

2.1. Sample collection and preparation

BrC samples for molecular characterization are collected with sufficient mass loadings of organic aerosol (OA) (approximately 100 μg or more) on various filter substrates such as Teflon, quartz fibers, or aluminum foil. This is done by sampling particulate matter (PM) from ambient air, test facilities, environmental chambers, and flow reactors using aerosol samplers such as filter cartridges, cyclone fractionators, and impactors. Typically, size-combined sampling is used to collect BrC OA samples, where air is drawn through a filter to capture particulate matter (PM). Virtual impactors are often placed upstream of the sampling line to enforce an upper size cutoff, such as $PM_{2.5}$ or PM_{10}. Size-selective sampling of BrC OA has also been performed using multistage cascade impactors.[51,57,76] In field studies, samplers are often positioned on rooftops, elevated platforms, and deployed on aircraft to collect ambient aerosol samples. In lab studies, samplers are directly interfaced with environmental chambers, flow reactors, and combustion test rooms. Some laboratory experiments testing BrC transformation mechanisms are performed directly on filters exposed to UV radiation or atmospheric gases.[98–102]

The BrC and other constituents of OA are extracted from filters by sonication[59,103,104] (or shaking)[105,106] into polar solvents such as water,[58,103,105,107] acetonitrile,[58,86,99,107] methanol,[104,108] and their mixtures.[51] Organic solvent mixtures with a broad range of polarity, such as acetonitrile/dichloromethane/hexane (referred to as 'orgmix' hereafter),[58,59,106,109] are used to further isolate polar and non-polar BrC components. Obtained extracts are

Open Access Article. Published on 02 January 2025. Downloaded on 1/23/2026 11:08:06 PM.
This article is licensed under a Creative Commons Attribution-NonCommercial 3.0 Unported Licence.

filtered through pre-wetted membrane syringe filters (PVDF or PTFE) to remove insoluble residues prior to HPLC–PDA–HRMS analysis, which could otherwise clog the system. When extracted into water, an additional purification step is required to remove dissolved inorganic salts, as high concentrations of inorganic ions suppress ionization of organic analytes. Inorganic salts also can precipitate in the presence of organic solvents used for LC separation. In C18 columns, inorganic ions coelute with other small polar organic analytes during the first few minutes, hindering quantification of these small organics. This issue is even more significant when using a column with polar characteristics or ion-exchange capabilities, as these can retain inorganic ions longer.[52,57] Solid-phase extraction (SPE) is often used to desalt aqueous extracts. SPE can also remove small organic acids, low molecular weight organosulfates, sugars, and highly oxidized small organic molecules that are too hydrophilic to retain on the C18 cartridge. Due to their small molecular size and limited contributions of double bonds, these species are either non-light-absorbing or exhibit only weak absorption, contributing minimally to BrC.[77,103,105,110] Often, water extracts are acidified to pH $\sim$ 2 prior to SPE purification to retain most of the water-soluble organics.[105]

Substantially higher fractions of organic carbon (OC) from aerosol samples are extracted into polar organic solvents rather than into water.[110–112] BrC consists of organic compounds with very diverse polarities, so a mix of organic solvents often results in the highest extraction efficiency.[58,59] Fig. 1 indicates that 'orgmix' is the most efficient solvent for extracting BrC from fresh, unaged biomass burning organic aerosol (BBOA).[58] On the other hand, atmospherically aged BBOA components enriched in various oxygenated and nitro groups are adequately extracted into water or polar organic solvents. In addition to filter sampling, BrC components of fog and cloud water are collected using cloud water collectors.[113,114] These samples can be directly analyzed by HPLC–PDA–HRMS after filtering out insoluble particles. However, the effects of incomplete extraction efficiency must always be considered for a thoughtful interpretation of BrC optical properties and composition measured in experiments.

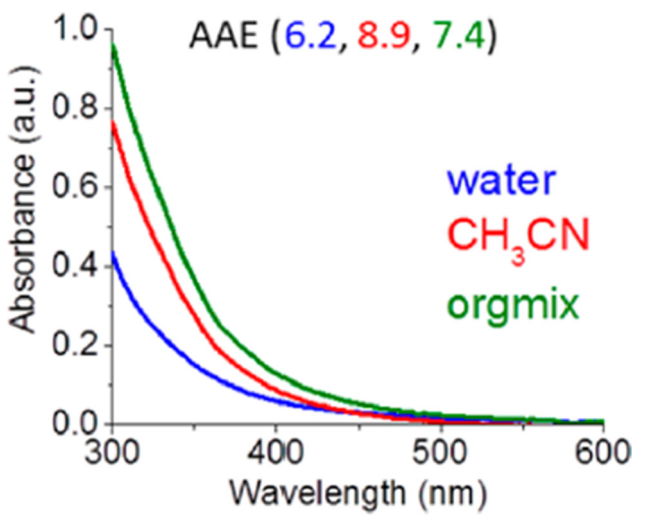

Fig. 1 UV-Vis spectra BrC solutions extracted with different solvents for the same BBOA sample. The amount of extracted BrC generally follows the trend: 'orgmix' > single polar solvent (acetonitrile, methanol) > water. Accordingly, the Absorption Ångström Exponent (AAE) values measured for BrC extracts tend to increase with higher extraction efficiency. Reproduced from ref. 58 with permission from the American Chemical Society, copyright 2017.

Desalting BrC extracts from common inorganic salts like ammonium sulfate (AS) can be facilitated by adding polar solvents (*e.g.*, acetonitrile, methanol) leading to liquid–liquid phase separation. When acetonitrile is added, the extract separates into two layers (organic-rich and salt-rich) due to the salting-out effect of AS.[53,99,115] Large AS loadings can also cause precipitation in addition to liquid–liquid phase separation. The organic-rich layer is then separated and used for analysis. Concentrated mixtures of BBOA analytes tend to self-separate over time into 'aqueous' and 'oil' fractions after prolonged storage.[76,107,116] These phase-separated fractions can be characterized separately.

Depending on the mass loadings and absorbance of the BrC extracts, samples may need to be further diluted or concentrated prior to HPLC–PDA–HRMS analysis to be consistent with the detection range of the PDA detector. Dilution is often performed with the same type of solvent or solvent mixtures used for extraction. Very diluted samples and those with no apparent color (pale yellow) often need to be pre-concentrated. For this, the organic solvent in sample extracts is evaporated under a light stream of pure nitrogen gas using an evaporator system[51,104] such as a turbovap or minivap. Low-level heating (around 40 °C) is commonly applied to evaporate water.[103] For better HPLC performance, samples are usually reconstituted in a solvent mixture matching composition of the initial mobile phase to improve analyte retention on the column. Alternatively, a different solvent miscible with both the extract and the initial mobile phase can be used to facilitate mixing and analyte retention on the column. For example, samples originally extracted in 'orgmix' solvent (not fully miscible with the aqueous mobile phase of LC) can be reconstituted in dimethyl sulfoxide before analysis to improve mixing with the mobile phase.[54,59,109]

2.2. Separations and optical detection of BrC components in environmental mixtures

Reverse phase liquid chromatography (RPLC) is the most common method for separating complex organic mixtures due to its ability to retain analytes across a wide range of polarities. RPLC uses a non-polar stationary phase, typically C18, and a gradient of aqueous (weak) and organic (strong; acetonitrile or methanol) mobile phases. Gradient separation, transitioning from low to high organic solvent, elutes more peaks in a shorter time compared to isocratic elution. Analytes elute in order of decreasing polarity: heavily oxygenated BrC chromophores elute first, while non-polar chromophores such as small polyaromatic hydrocarbon (PAH) species elute last.[59,76] However, high molecular weight PAHs (>400 Da) may not elute using this protocol, preventing their detection in HPLC–PDA–HRMS.[59] Trace additives like acetic

 This journal is © The Royal Society of Chemistry 2025

Open Access Article. Published on 02 January 2025. Downloaded on 1/23/2026 11:08:06 PM.
This article is licensed under a Creative Commons Attribution-NonCommercial 3.0 Unported Licence.

and formic acid enhance retention of acidic compounds and facilitate formation of protonated analyte ions in the (+)ESI mode. It is important to note that pH can modify the absorption spectra of BrC chromophores. For instance, deprotonated nitrophenols absorb at longer wavelengths than their neutral forms.[51,58] In contrast, deprotonated benzoic acid and their derivatives,[117] protonated amines,[113] and imidazoles[18] absorb at shorter wavelengths than their neutral species. Measuring absorbance under acidic conditions is more atmospherically relevant since ambient aerosols are typically acidic (pH 1–5).[118]

Optimized chromatographic separation is crucial for detecting many BrC chromophores. Fig. 2 illustrates the evaluation of six HPLC columns tested for separating BrC products formed in aqueous-phase reactions of methylglyoxal (MG) and ammonium sulfate (AS).[52] In this system, major BrC chromophores are organic species containing reduced nitrogen (N) moieties. An isocratic separation at 20 : 80 water–acetonitrile was used in HILIC, while gradient separation with water and acetonitrile was used with other columns. The commonly used 'C18 Luna' and polar embedded 'C18 Fusion' columns show poor separation of positively charged reduced N chromophores, such as imidazole and pyrroles. In contrast, the 'SM-C18' column, which has ion exchange capabilities in addition to reversed phase interactions, performs the best separation for this mixture. However, SM-C18 also retains inorganic ions, suppressing ESI-HRMS detection, making desalting crucial. 'Biphenyl' and 'C18 Hydro' columns provide better separation compared to 'C18 Luna' and 'C18 Fusion,' but their performance is inferior to 'SM-C18.' The least efficient separation is observed with the HILIC column due to the relatively low polarity of these analytes. Therefore, selecting an appropriate stationary phase is essential for improving the separation of BrC mixtures.

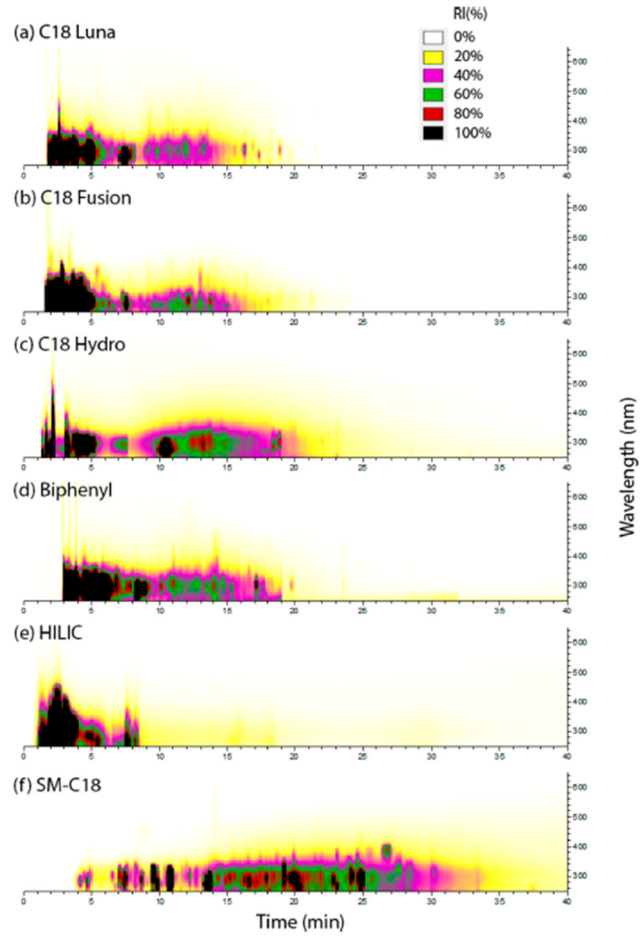

Fig. 2 HPLC–PDA chromatograms of laboratory generated BrC species formed by the aqueous-phase reactions of methylglyoxal (MG) and ammonium sulfate (AS), separated on six HPLC columns. Reproduced from ref. 52 with permission from the American Chemical Society, copyright 2016.

HPLC systems are commonly equipped with a photodiode array (PDA) detector that measures light absorption by eluted compounds at selected wavelengths or across a broad spectral range. Often, 365 nm is used as an indicator of BrC absorption.[108,119,120] However, HPLC–PDA alone cannot unambiguously identify BrC species in untargeted analysis, necessitating the integration of an HRMS detector, which facilitates the determination of their elemental and possibly structural composition. The effluent flow from the HPLC is either split between the PDA and the HRMS or, most commonly, sent sequentially through the PDA first, followed by the HRMS. Regardless of the configuration, there is a time shift between detection by the PDA and HRMS. After correcting for the time shift, eluted components can be identified based on their UV-vis spectra recorded by the PDA and their chemical composition inferred from the HRMS.

Quantitative analysis of HPLC–PDA records for BrC extracts with known OC injected mass allows calculation of the wavelength-dependent mass absorption coefficient ($\mathrm{MAC}(\lambda)_{\mathrm{BrC}}$) of the extracted BrC mixture and the corresponding contributions of its individual prominent chromophores ($\mathrm{MAC}(\lambda)_i$).[76,80] Typically only 40–60% of the $\mathrm{MAC}(\lambda)_{\mathrm{BrC}}$ value can be attributed to the identifiable prominent chromophores ($\sum \mathrm{MAC}(\lambda)_i$).[40,54,76,121,122] The remaining 'unassigned' fraction of light absorption corresponds to a combined effect of unseparated BrC chromophores, minor chromophores, and possible intermolecular interactions such as the formation of charge transfer complexes[123] between co-eluting organic compounds.[57] A rising baseline or a broad hump in the middle of the HPLC runs is commonly observed in the analysis of complex organic mixtures.[51,86,110,119,124] These are usually attributed to the coelution of many poorly separated species, which can be either weak chromophores or strong chromophores at low concentrations. Further separation and identification of these coeluting chromophores could be achieved using two-dimensional (2D) HPLC separation employing columns with different stationary phases, such as HILIC and RPLC, allowing more complete orthogonal separation of polar and non-polar components of complex organic mixtures.[81,116,124] For rapid, high-level assessments and comparisons of BrC components across various samples, a practical fractionation method can be utilized.[66,75] This method involves categorizing 3–4 groups of species based on their LC elution fractions, correlating the abundance of these groups with their contributions to light absorption, and linking these results to their group-specific composition inferred from HRMS data. This approach has been

Open Access Article. Published on 02 January 2025. Downloaded on 1/23/2026 11:08:06 PM.
This article is licensed under a Creative Commons Attribution-NonCommercial 3.0 Unported Licence.

employed to characterize the biofuel-specific molecular features of BrC produced from different biomass burnings[66] and to study the chemical transformations and darkening trends in evaporating BBOA.[75]

2.3. Use of different ionization modes

The chemical composition of BrC chromophores is diverse, spanning molecules from various chemical classes with different polarities.[59,125] These include polar organics (*e.g.*, carboxylic acids, esters, nitro-organics), semi-polar organics (*e.g.*, phenolic acids, lignin fragments, substituted aromatics, organosulfates), and nonpolar compounds (*e.g.*, PAHs, O-, N-heterocyclic PAHs). Inherent to this variability, efficient detection by HRMS requires multiple ionization schemes and polarity modes.[66,75–77,101,125–127] Fig. 3 shows direct infusion HRMS spectra of the same BBOA BrC analyte mixture ionized by electrospray ionization (ESI) and dopant-assisted atmospheric pressure photoionization (APPI) sources in positive (+) and negative (−) modes.[59] The mass spectra differ significantly among the four ionization schemes. The (+)ESI mode detects analytes with higher molecular weights (MW > 500 Da) than the (−)ESI and (±)APPI modes. APPI modes detect a larger fraction of organic compounds, about 80% of the total species identified. Each mode preferentially ionizes specific subclasses of BBOA components, showing molecular selectivity. Because of the diversity of atmospheric BrC chromophores, datasets from ESI and APPI modes show minimal overlap,[65,127] with less than 10% of species detected in both modes.

Differences between ESI and APPI datasets are additionally influenced by the varying composition of HPLC solvents at different elution times. ESI effectively ionizes polar and semi-polar compounds with acidic (negative mode) and basic (positive mode) functionalities through charge competition among analytes in the ESI spray droplets. BrC chromophores with CHO composition, related to various phenolic compounds and their oligomers, can be detected in both positive and negative ESI modes as $[M + H]^+$, $[M + Na]^+$, and $[M–H]^-$ ions. Sodium formate adduct ions $[M + (HCOONa)_x–H]^-$ are common when the LC mobile phase contains formic acid for modifying pH.[122,128,129] BrC chromophores with CHON composition are typically detected as $[M–H]^-$ ions when they contain nitro ($–NO_2$) and nitrate ($–NO_3$) groups,[40,51,130,131] while those with reduced N moieties (*e.g.*, Schiff bases, N-heteroatom aromatics, imines) are observed as $[M + H]^+$ ions.[52,59,100,109] Low-polarity BrC chromophores like PAHs and their derivatives may appear in the (+)ESI mode as $[M + H]^+$ and radical cations $[M]^{\bullet+}$.[54,76,80,106,109] APPI efficiently ionizes aromatic nonpolar and low-charge affinity species through electron detachment, charge-exchange, and proton-transfer reactions between dopant molecules and ions in the plume,[132,133] typically forming $[M]^{\bullet+}$ ions of analyte. APPI offers significant advantages, including minimal ion suppression in complex mixtures, higher sensitivity, and a larger linear dynamic range compared to ESI.[80,133,134] Fig. 4 shows common chemical classes of BrC species detected in a BBOA sample, depicted as annotated features on the HPLC–PDA heatmap (panel a), and selected ion chromatograms (SICs) reporting chromophore-specific ions detected in (−)ESI, (+)ESI, and (+)APPI modes (panel b).[59] Polar phenolic and nitrophenolic chromophores elute first, with abundant HRMS features detected in (−)ESI mode. Less polar O-PAH and N-PAH heterocyclic chromophores elute next, mostly observable in (+)ESI mode. Finally, non-polar PAH chromophores ionizable in (+)APPI elute last. Therefore, molecular characterization of BrC samples typically requires sequential multi-modal HRMS analysis with different ionization schemes.[59,66,75–77,101,125–127]

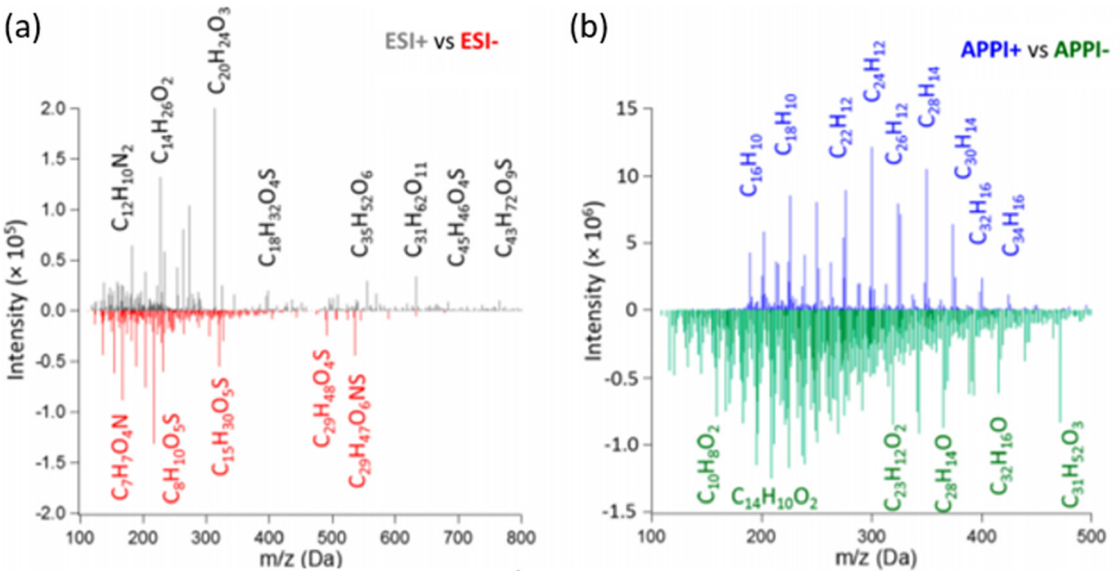

Fig. 3 HRMS detection of solvent-extractable BBOA components assisted with electrospray ionization (ESI) and dopant assisted atmospheric pressure ionization (APPI), with spectra recorded in positive (+) and negative (−) polarities, respectively. Molecular formulas correspond to neutral molecules. Peak intensities are plotted as positive and negative features reflecting polarity of the detected ions. Reproduced from ref. 59 with permission from the American Chemical Society, copyright 2018.

 This journal is © The Royal Society of Chemistry 2025

Open Access Article. Published on 02 January 2025. Downloaded on 1/23/2026 11:08:06 PM.
This article is licensed under a Creative Commons Attribution-NonCommercial 3.0 Unported Licence.

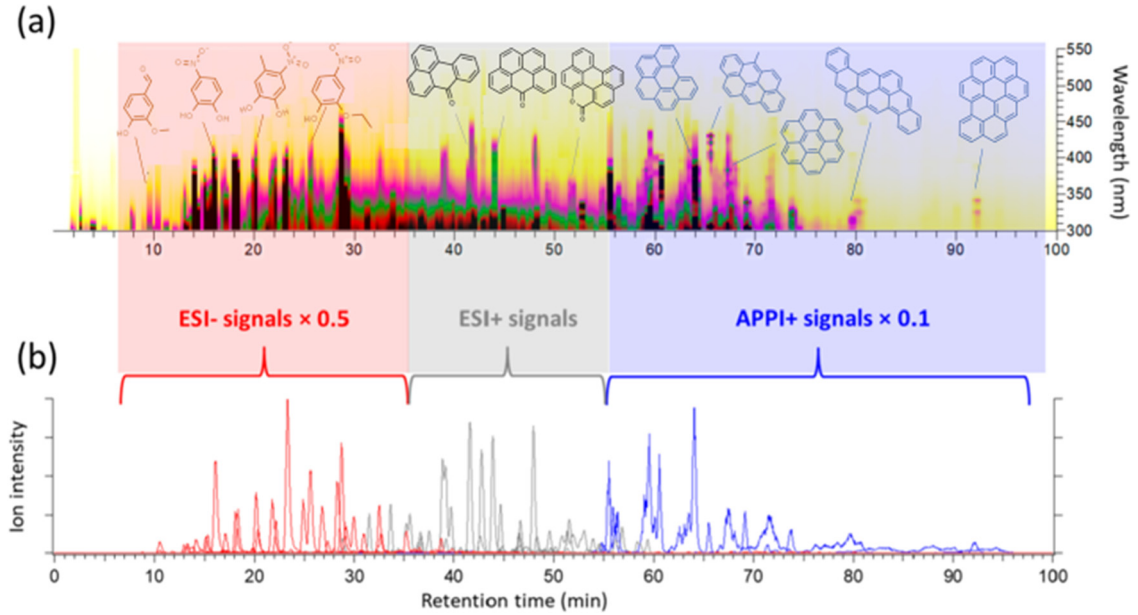

Fig. 4 HPLC–PDA (a) and HPLC–HRMS (b) chromatograms of a BBOA sample. The *y*-axis and color map in panel (a) refer to the wavelength and the UV-vis absorbance, respectively. Selected UV-vis features are annotated with molecular structures of the identified BrC chromophores. Panel (b) shows cumulative ion intensity of the selected ion chromatograms (SIC) corresponding to BrC chromophores detected in (+)ESI, (−)ESI and (+)APPI modes, respectively. Reproduced from ref. 59 with permission from the American Chemical Society, copyright 2018.

2.4. Untargeted analysis, interpretation of HPLC–PDA–HRMS data for BrC studies

Untargeted analysis of complex OA mixtures containing BrC species is laborious, requiring statistical, data-processing, and visualization tools to extract meaningful results from multi-dimensional datasets. Open-source programs such as MZmine,[135,136] XCMS,[137] and DeconTools[138] help process raw data files, reduce mass spectral data, construct SIC profiles, deconvolute spectral features, align chromatographic features, de-isotope HRMS spectra and propose elemental formulas for detected ions, visualize data in Kendrick mass defects (KMD)[139] and Van Krevelen plots.[140] Formula assignment in HRMS data is traditionally assisted by KMD analysis, which identifies groups of homologous compounds differing only by a number of base units such as CH_2, H_2, O, CH_2O, *etc.*[139,141] Higher-order KMD analysis extends this concept to multiple base units, enabling grouping into higher-order homologous series containing species with compositional differences defined by two or three base units.[141] This approach greatly simplifies visualization of complex mass spectra and increases the number of assigned elemental formulas. Identifying a single organic compound in one group helps determine the elemental formulas for all group members.[59]

Correlating HRMS-identified compounds eluted at certain retention times with corresponding UV-vis spectra recorded by the PDA detector presents another challenge. Time-shift corrected HPLC–HRMS and HPLC–PDA signals of eluting chromophores are correlated based on LC peak width, peak shape, and molecular ion abundance.[52,57,59,76] Chemical identity of BrC chromophores can be suggested based on the features of their UV-vis and HRMS spectra, referenced to existing literature reports,[142] spectral databases (*i.e.* NIST, ChemSpyder, *etc.*), theoretical calculations,[87,143] educated guesses, and based on the analysis of relevant commercial standards. Determining molecular structures of BrC species with greater confidence often requires additional experimental (*i.e.* tandem MS^n) and data analysis methods.[80,122,144]

Rapid assessment of potential BrC chromophores among identified molecules can be inferred from double bond equivalent (DBE) values, which reflect the degree of potential conjugation in organic molecules. Fig. 5 shows DBE values plotted *versus* the number of carbon atoms in BBOA components based on HRMS measurements.[59] Reference lines depict DBE values characteristic of fullerene-like hydrocarbons,[145] *cata*-condensed PAHs,[146] and linear polyenes (C_xH_{x+2}).[147] Compounds with a DBE/C ratio greater than the polyene line are potential BrC chromophores, with light absorption capability increasing as DBE/C values approach the fullerene-like limit.[59] The shaded region in the DBE *vs.* C plot highlights potential BrC chromophores, while compounds below the polyene line have more aliphatic moieties and contribute less to visible light absorption. The most absorbing BrC chromophores, with high DBE/C and high molecular weight, contain longer networks of aromatic and conjugated π-bonds and are well ionized by APPI, making it the method of choice for sensitive and selective detection of BrC species.[73]

3. Characterization of BrC species in environmental samples

3.1. Atmospheric aerosols

Primary BrC from BBOA emissions significantly impact air quality and climate radiative forcing on regional and global

Open Access Article. Published on 02 January 2025. Downloaded on 1/23/2026 11:08:06 PM.
This article is licensed under a Creative Commons Attribution-NonCommercial 3.0 Unported Licence.

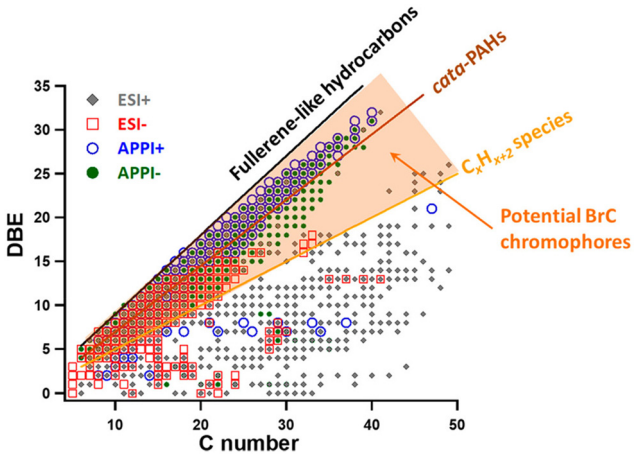

Fig. 5 DBE *vs.* number of Carbon atoms in the HRMS identified individual components of BBOA sample detected in each of the (±)ESI an (±)APPI ionization modes. Reproduced from ref. 59 with permission from the American Chemical Society, copyright 2018.

scales. High levels of BrC light absorption have been reported in South America and Central Africa during wildfire seasons.[12,14,148] Because of the global warming, wildfire occurrences and intensities are increasing worldwide, affecting new areas such as Southeastern and Western USA, Canada, Australia, and boreal regions of Russia, Canada, and Alaska.[149–153] Additionally, in densely populated areas of India and China, BrC emissions are primarily from coal and biofuel[12] used for heating during winter.[148] Secondary BrC species from various anthropogenic emissions further contribute to urban areas in North America and Europe.[12] The light absorption properties of BrC depend on the molecular composition and concentration of chromophores, which vary based on sources, locations, and pollution levels.

An early HPLC–PDA–HRMS study[105] compared BrC species detected in atmospheric water-soluble humic-like substances (HULIS) from different emission sources: an urban site influenced by traffic (Budapest, Hungary), a rural site dominated by plant emissions (K-puszta, Hungary), and an Amazonian Forest site affected by fires (Rondônia, Brazil). Samples attributed to BBOA emissions exhibited the most visible brownish color, due to high concentrations of nitroaromatics like 4-nitrocatechol and methyl nitrocatechols, which absorb strongly at 350–360 nm and tail into the 420–430 nm range. The highest concentrations of these chromophores were found in smoldering fire emissions, with lower levels in flaming fires and urban aerosols.[105] This study highlighted the significance of nitroaromatic compounds (NAC) as BrC chromophores and their variation due to differences in biofuel composition, burning conditions, and diurnal chemistry.[19] Later studies confirmed the importance of NAC in both BBOA[58,122] and anthropogenic POA/SOA.[40,51]

Substantial fractions of BrC in ambient samples are not water-soluble and require solvent extraction. In Pasadena, CA, methanol-soluble BrC absorbed four times more light at 365 nm than water-soluble BrC, attributed to local traffic emissions.[119] Similarly, in samples collected at urban sites in Xian and Beijing, water-insoluble BrC contributed over 50% of light absorption during winter.[110] BrC species in water-soluble (WS) and water-insoluble (WI) fractions revealed PAHs and oxy-PAHs with 4–6 aromatic rings in WI, and common NAC and oxygenated O-PAHs with 2–3 rings in WS.[110] These results indicated that significant BrC absorption in urban aerosol could be attributed to individual chromophores identifiable by HPLC–PDA–HRMS.

Seasonal variations in water-soluble BrC in Beijing, China, revealed selected NAC specific to winter and summer.[85] Many winter-specific NAC BrC species matched components from SOA generated in laboratory experiments simulating high NO_x photooxidation of toluene, benzene, and phthalic acid related to coal combustion. Summer-specific NAC BrC species indicated biomass burning influence. This seasonal variation reflects different BrC sources: BBOA in summer and coal combustion and anthropogenic SOA in winter. Trends in BrC chromophores on polluted and less polluted days showed dinitro aromatic compounds on polluted days and reduced nitrogen species on less polluted days. Nitrophenols and methyl nitrophenols were higher on less polluted winter days, while nitrocatechols were higher on polluted winter days, attributed to differences in VOC precursors and oxidant concentrations affecting SOA formation and aging.

Comparing methanol-extracted BrC from winter aerosol samples in urban (Beijing) and rural (Dezhou) China showed many common chromophores, despite different emission influences: vehicle emissions in Beijing and biomass burning in Dezhou.[154] Total BrC light absorption in Dezhou was about twice that in Beijing. Twenty-nine common chromophores contributed 25% and 22% of total absorption in Beijing and Dezhou, respectively, with a UV-vis absorption maximum around 320 nm. Major contributors to light absorption (>80%) and mass concentrations (>40%) at both sites were 4-nitrocatechol, 4-nitrophenol, and derivatives. Nitrophenols absorb strongly around 310–330 nm, and nitrocatechols around 340–350 nm due to an additional –OH group. Phthalic acid, an anthropogenic SOA tracer, was higher in Beijing, while pyrocatechol, nitroguaiacol, and methyl catechol related to BBOA were higher in Dezhou. Fig. 6 shows catechol absorption enhancement due to NO_2 replacement and rearrangement to 4-nitrocatechol. Aromatic compounds with multiple functional groups, such as acetosyringone and ferulic acid, have comparable absorptivity to 4-nitrophenol despite lower concentrations. Average concentrations of common BrC chromophores were higher in Dezhou (302 ng m^{-3}) than Beijing (112 ng m^{-3}), except on high pollution days. Mass fractions of NAC BrC species were only 0.25% and 0.32% of total aerosol mass in Beijing and Dezhou, respectively. Strong positive correlations between BrC absorbance and NO_x concentrations suggest that reducing NO_x will also reduce BrC.

Substantial contributions of NAC to total BrC absorption by BBOA have been reported in additional studies from various locations. Analysis of acetonitrile-soluble $PM_{2.5}$ extracts from a research vessel on the Yangtze River between Shanghai and Wuhan showed that NAC species contributed ~25–27% at

 This journal is © The Royal Society of Chemistry 2025

Open Access Article. Published on 02 January 2025. Downloaded on 1/23/2026 11:08:06 PM.
This article is licensed under a Creative Commons Attribution-NonCommercial 3.0 Unported Licence.

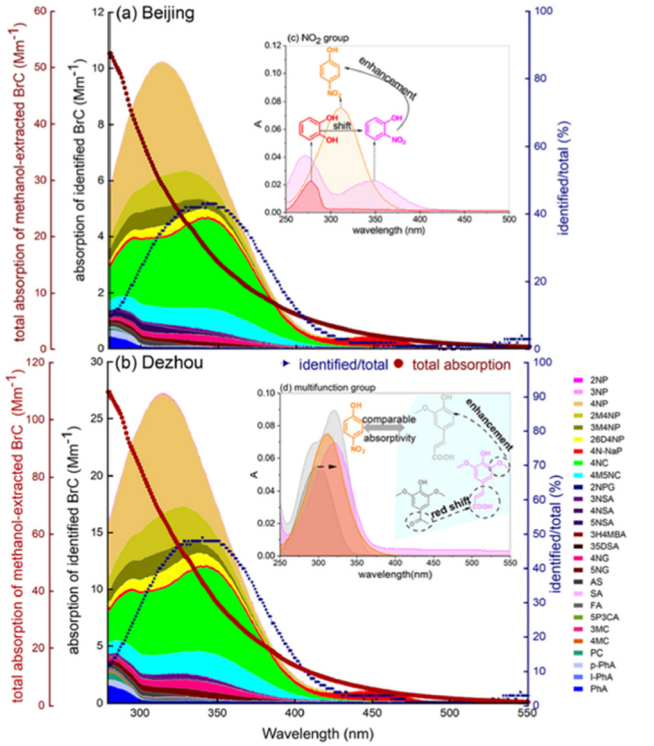

Fig. 6 Absorption by BrC and its individual species measured at (a) Beijing urban site influenced by traffic emissions and (b) Dezhou site influenced by BBOA emissions. Wine red lines show total BrC absorption. Stacked colored areas indicate contributions by identified individual BrC species. Blue lines show ratios of identified/total absorption. Insert (c) illustrates influence of $-NO_2$ group on the absorbance of phenols. Insert (d) illustrates effects of $-NO_2$ and various other functional groups on the absorbance of phenols. Reproduced from ref. 154 with permission from Elsevier, copyright 2021.

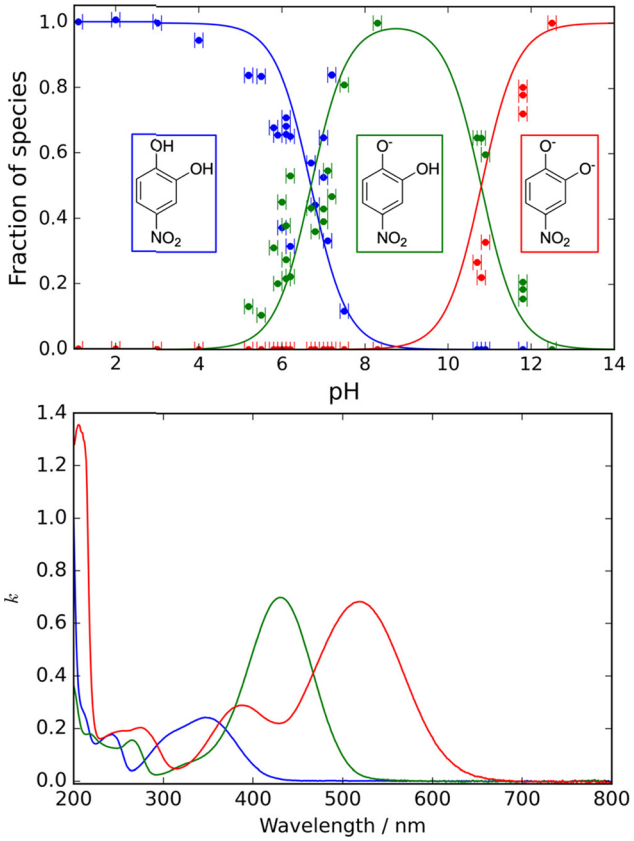

Fig. 7 Upper panel: pH-Dependent fractions of 4-nitrocatechol (4NC), singly deprotonated ($4NC^-$), and doubly deprotonated ($4NC^{2-}$) ions. Data points represent experimental values obtained *via* UV/visible spectroscopy, while the lines correspond to equilibrium calculations based on literature-reported pK_a values. Lower panel: Wavelength-dependent imaginary refractive indices for individual 4NC, $4NC^-$, and $4NC^{2-}$ species, highlighting their distinct optical absorption characteristics. Reproduced from ref. 155 with permission from the American Chemical Society, copyright 2024.

290 nm and 55–65% at 350 nm of the BrC absorption.[86] The most significant contributors were nitrophenols, followed by other nitroaromatics. Additional strong chromophores included benzoic acid, benzyloxy benzonitrile, oxygenated polycyclic aromatic hydrocarbons (O-PAHs), and their derivatives. Altogether, the 13 most absorbing chromophores contributed nearly half of the BrC absorption. A broad range of weakly absorbing species and trace components highlighted BBOA as the major source of BrC in the study area. Similarly, significant NAC contributions to BrC absorption (~20% at 300 nm, ~50% at 350–475 nm, and ~80% at 500 nm) were reported for water soluble fractions of BBOA samples collected during a bonfire festival in Israel.[58]

Aerosol acidity is a key factor in determining the light absorption of NAC and other chromophores.[43] Conversion of neutral NAC into their anionic forms at neutral pH shifts BrC absorbance from UV to visible wavelengths. For example, Fig. 7 illustrates the fractional distribution of undissociated 4-nitrocatechol (NC) and its ionic forms, singly deprotonated ($4NC^-$) and doubly deprotonated ($4NC^{2-}$), in aqueous solution as a function of pH, alongside their corresponding wavelength-dependent imaginary refractive indices.[155] At the typical acidity of atmospheric aerosols and cloud droplets (pH < 6), 4NC and $4NC^-$ are the predominant species. Notably, $4NC^-$ exhibits stronger BrC absorption than 4NC, with red-shifted absorption bands. Under acidic conditions (pH < 4), BrC absorption is primarily driven by 4NC and is relatively weaker. In contrast, at near-neutral pH (6–7), BrC absorption intensifies and becomes highly dependent on the fraction of $4NC^-$ ions. Similarly, Fig. 8 demonstrates that other common BrC chromophores, such as imidazoles and N-containing oligomers formed *via* aqueous-phase atmospheric reactions between α-dicarbonyls and amines or ammonium,[156] exhibit a comparable pH-dependent trend, with enhanced light absorption observed at near-neutral pH.[157] The results of these targeted laboratory studies indicate that BrC formation and its light-absorbing properties are significantly influenced by aerosol and cloud droplets pH, with neutral to mildly alkaline conditions (pH 6–8) promoting these processes. Such conditions are often associated with elevated concentrations of ammonium, amines, and alkaline cations like Ca^{2+} from dust. These findings highlight the critical role of pH-driven effects on BrC formation and absorption, particularly in regions where aerosols frequently exhibit neutral pH, such as northern China.[158–161]

Open Access Article. Published on 02 January 2025. Downloaded on 1/23/2026 11:08:06 PM.
This article is licensed under a Creative Commons Attribution-NonCommercial 3.0 Unported Licence.

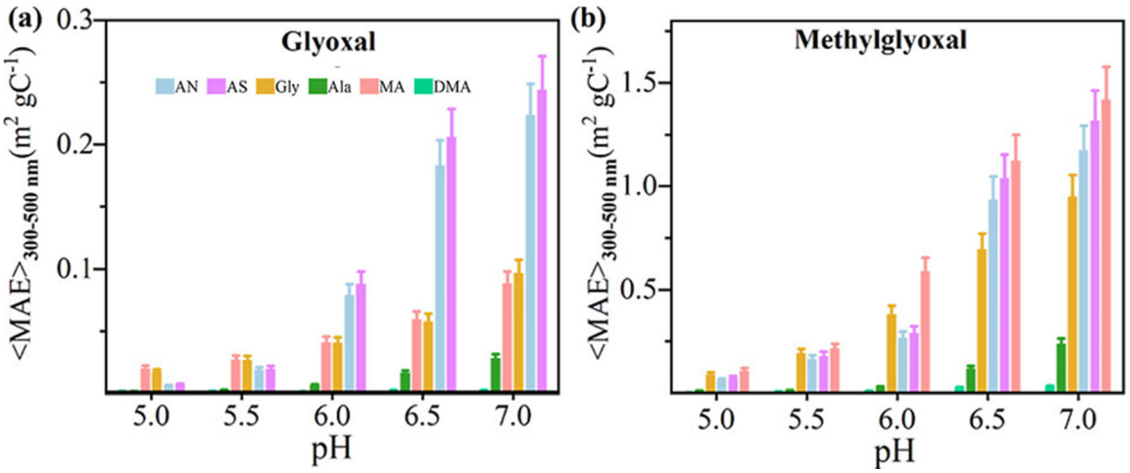

Fig. 8 Average mass absorption coefficients (or efficiency, MAE, as labeled in this plot) integrated over the 300–500 nm wavelength range reported for BrC mixtures formed from reactions of (a) glyoxal and (b) methylglyoxal in aqueous solutions containing ammonium nitrate (AN), ammonium sulfate (AS), glycine (Gly), alanine (Ala), methylamine (MA), and dimethylamine (DMA), demonstrating enhanced BrC absorption at near-neutral pH conditions. Reproduced from ref. 157 with permission from the American Chemical Society, copyright 2024.

In line with the pH dependence observed in laboratory BrC proxies, BrC components in BBOA from field studies exhibit similar trends. Fig. 9 shows UV-vis spectra of water soluble BrC at acidic (pH = 3) and neutral (pH = 7) conditions.[58] The subset shows absorption of the same BrC sample extracted into water, acetonitrile, and a solvent mix, indicating that BrC chromophores do not dissociate in pure organic solvents and their light absorption properties remain as neutral species. Therefore, reporting MAC values of atmospheric BrC and their practical parameterization for models need to consider aerosol acidity. Since atmospheric aerosol is typically acidic, using low pH conditions is more practical to assess light absorption by water soluble BrC. Additionally, it is more convenient to extract ambient aerosols into an organic solvent or a mixture of organic solvents to accommodate BrC species with different polarities.

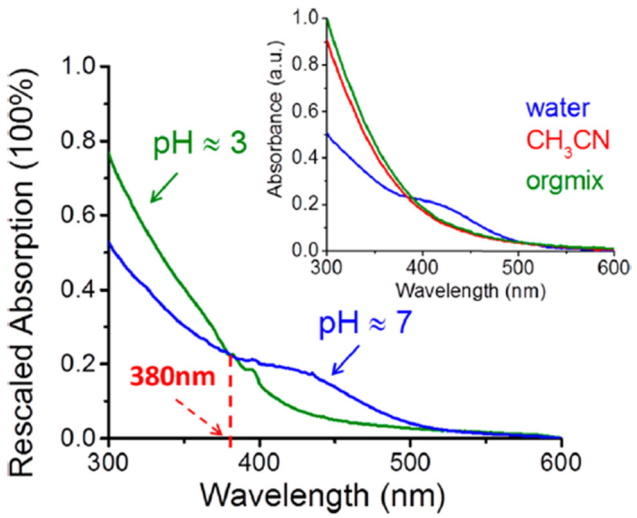

Fig. 9 UV-vis spectra of water extractable BrC recorded at different pH conditions. The insert shows spectra of the BrC extracted with different solvents from the same sample. Reproduced from ref. 58 with permission from the American Chemical Society, copyright 2017.

NAC species are dominant BrC chromophores in aged BBOA aerosol, especially when influenced by urban environments where common high-NO_x conditions favor the formation of nitro-phenolic compounds during daytime $^{\bullet}OH$-driven photooxidation of aromatic hydrocarbons.[51] Nighttime chemistry, driven by $^{\bullet}NO_3$ and O_3, also contributes to the nitration of aromatic compounds, enhancing BrC properties.[39] Fig. 10 highlights a field study from Israel where a biomass-burning event during a national festival allowed for the study of nighttime chemical evolution of BB aerosol.[162] NAC chromophores, such as 4-nitrophenol, 4-nitrocatechol, 4-nitrosyringol, oxidation-nitration products of methoxyphenols (MOPs), and lignin pyrolysis products, contributed significantly to BrC light absorption during and after the event.[58] The study found that $^{\bullet}NO_3$-driven nighttime chemistry played a key role in the aging of BBOA and its BrC properties. In fresh BBOA, BrC species are typically aromatic compounds with multiple hydroxyl/methoxy and aldehyde/ketone groups,[57,76] consistent with lignin pyrolysis fragments.[163] Similarly, in urban Singapore, NAC chromophores were abundant during Indonesian peatland fire episodes, along with lignin fragments like ferulic acid, *p*-coumaric acid, and coniferaldehyde.[104] Across field observations, identified BrC species contribute moderately to OA mass fractions (<10%) but significantly influence the overall light-absorbing properties of OA.

3.2. Cloud and fog water, snowpack deposits

Throughout their atmospheric lifetime airborne OA particles become immersed in water droplets of fogs and clouds, where in-cloud photochemistry and aqueous processing of water-soluble organics modify composition and properties of original and secondary formed BrC species. Wet and dry deposition

 This journal is © The Royal Society of Chemistry 2025

Open Access Article. Published on 02 January 2025. Downloaded on 1/23/2026 11:08:06 PM.
This article is licensed under a Creative Commons Attribution-NonCommercial 3.0 Unported Licence.

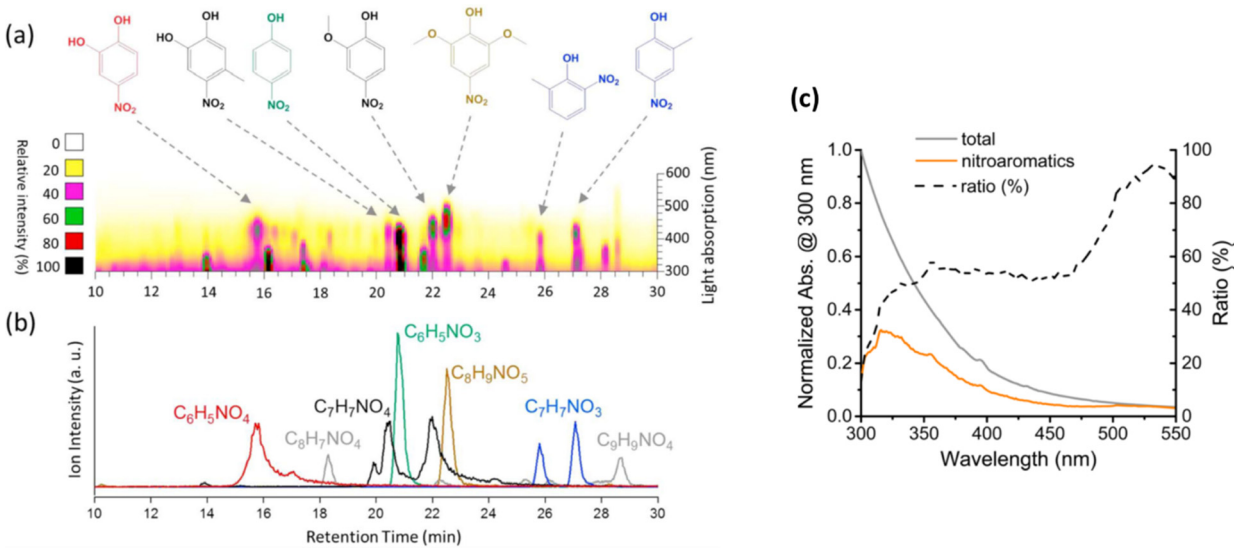

Fig. 10 (a) HPLC–PDA chromatogram of BrC collected during biomass burning event related to national festival in Israel. (b) Selected ion chromatograms (SIC) corresponding to most absorbing BrC chromophores identified by (−)ESI-HRMS. (c) Contribution of identified NAC (orange solid) to the total light absorption by BrC (gray solid); dashed line shows the ratio of identified/total absorption *versus* wavelength. Reproduced from ref. 162 (panels a, b) and ref. 58 (panel c) with permissions from Elsevier and the American Chemical Society, copyright 2017.

of BrC on snow and glaciers reduces albedo, influencing environmental and climatic feedback. HPLC–PDA–HRMS analysis of atmospheric water and snow samples provides crucial insights into the sources and dynamic changes in BrC composition and its light-absorption properties. An analysis of cloud water and rain samples from Mt. Tai, North China Plain, collected during episodes of aged agricultural BB emissions, identified 16 major BrC chromophores, primarily NAC species dominated by 4-nitrophenol.[113] These species contributed to 48% of the total light absorption in the 300–400 nm range. Additionally, 65 minor BrC chromophores with weaker absorbance were identified, the majority being aromatic with 1–2 nitrogen atoms. Combined, these chromophores accounted for more than two-thirds of the total light absorption in the 300–400 nm range.

In northern Xinjiang, China, molecular characterization of WSOC and its BrC components in seasonal snow samples revealed diverse BrC sources, including atmospheric deposition, plant degradation, soil contributions, and microbial sources.[77,126,127] An HPLC–PDA–HRMS study of snowpack samples from various field sites detailed the molecular composition of BrC chromophores, highlighting the molecular-specific absorption properties of snowpack BrC for the first time. Five major types of snow BrC chromophores were reported: (1) phenolic/lignin-derived compounds, (2) nitroaromatics, (3) oxygenated aromatics, (4) flavonoids, and (5) other chromophores.[77] The first three types were the most light-absorbing in urban and polluted samples. Chromophores in remote snow samples exhibited distinct UV-vis features attributed to flavonoids. Identified chromophores accounted for ~23–64% of the total BrC light absorption in the 300–370 nm range. These studies[77,126,127] provided a comprehensive report on various BrC chromophores in midlatitude seasonal snowpack and their roles in snow radiative balance and photochemistry, warranting further research.

3.3. Biomass burning aerosol generated in laboratory settings

The chemical composition and optical properties of BBOA BrC depend on biomass type, burning conditions, and chemical aging. Numerous HPLC–PDA–HRMS studies have analyzed BBOA from test burns of various biofuels in controlled laboratory settings to distinguish common and biofuel-specific BrC chromophores.[57,66,76,104,106,109] One early study examined BBOA from controlled burns of sawgrass, peat, ponderosa pine, and black spruce, representative of different fire environments.[57] Identified BrC components exhibited different ranges of their molecular sizes and polarity characteristics across four tested samples. The most distinct sample from the sage burn showed abundant NAC species and less polar polyaromatic BrC chromophores like O-PAHs and N-PAHs. NAC and PAHs each contributed 25% of the total BrC absorption in that sample, while the remaining 50% was due to numerous weakly absorbing chromophores and intermolecular interactions. BrC species in the other three samples were dominated by monoaromatic compounds with oxygenated functional groups such as vanillin, derivatives of coumarin and xanthon, and larger pyrolysis products of lignin. While many of these species were common to all three samples, they varied in relative abundances and contribution to total BrC light absorption. Most BrC species detected in the samples from ponderosa pine and black spruce burns were similar in composition and contribution to total BrC light absorption, consistent with both biofuels belonging to coniferous trees. Significant differences in burning intensities were also observed, with sawgrass burns exhibiting highly flaming conditions. The study concluded that BrC composition and concentrations are influenced by both biomass type and the burning conditions.[57]

Open Access Article. Published on 02 January 2025. Downloaded on 1/23/2026 11:08:06 PM. This article is licensed under a Creative Commons Attribution-NonCommercial 3.0 Unported Licence.

Another HPLC–PDA–HRMS study investigated BBOA originated from gymnosperm (pines, firs) and angiosperm (sagebrush, ceanothus, chamise) biofuels burned under controlled flaming and smoldering conditions.[106] Common BrC chromophores included lignin pyrolysis products (sinapaldehyde, coniferaldehyde), plant secondary metabolites (coumarins, flavonoids), NAC, and PAHs. Sinapaldehyde and coniferaldehyde were dominant in angiosperm and gymnosperm BBOA, respectively. Vanillic acid was prevalent in conifer smoke, while veratraldehyde was common in both biofuel types. Major NAC chromophores were abundant in flaming fires of both types, and PAHs were particularly high in angiosperm flaming smoke.[106] A focused study on smoldering peat fires in Indonesia, a significant source of regional BrC, characterized BBOA from peat, fern, leaves, and charcoal.[104] Unlike other studies, individual chromophores did not dominate BrC absorption. Common chromophores included oxygenated monoaromatics (*e.g.*, ferulic and homovanillic acids, ethyl guaiacol), with NAC chromophores being less common but still detectable. Unique to peat BBOA were minor S-containing chromophores.[104] In rural India, where firewood, crop residues, and dung are commonly used for cooking and heating, a study characterized BBOA from burning brushwood and dry dung in cookstoves. The most abundant BrC chromophores were lignin pyrolysis products (*e.g.*, syringol, vanillic and homovanillic acids, syringealdehyde), with NAC chromophores more specific to brushwood.[109] Another study investigated BrC components in smoldering BBOA produced during smoke chamber experiments using common sub-Saharan African fuels, including hardwoods, cow dung, savanna grass, and leaves, and correlated these with field BBOA samples collected in Botswana.[79] In total, 182 individual BrC components were identified and classified into groups such as lignin pyrolysis products, nitroaromatics, coumarins, stilbenes, and flavonoids. Variations in BrC composition were correlated with optical absorption data obtained from an aethalometer, which collects aerosol samples on a filter tape and measures light attenuation through the filter. The aethalometer's multi-wavelength attenuation data enables real-time quantification of $MAC(\lambda)_{BrC}$ values, along with estimates of BC and BrC mass concentrations,[164–166] capturing variations due to emission sources and atmospheric aging. Combining these optical measurements with molecular characterization, the study found a linear relationship between the contribution of identified BrC species to the BBOA mass (0.4–14%) and their MAC $(370\ nm)_{BrC}$ values (0.2–2.2 $m^2\ g^{-1}$).[79] Collectively, the findings from these studies underscore how factors such as biomass type, combustion conditions, and aging processes influence both the chemical composition and optical properties of BrC in BBOA.

A recent study investigated BrC species in BB smoke condensates generated from heated hardwood pellets, simulating oxidative and pyrolysis conditions.[76] The collected condensates exhibited phase separation into 'darker oily' and 'lighter aqueous' immiscible phases. Fig. 11 illustrates the distinct BrC features in the oily (PO) and aqueous (PA) phases.[39] Both phases contained common polar monoaromatic species and lignin pyrolysis products. However, BrC components of PO were dominated by less polar diterpenoids and non-polar substituted PAHs. The physicochemical properties of BrC species indicated that the species in PO are less volatile and more viscous compared to the common BrC chromophores. These results suggest that atmospheric BrC may darken as high-volatility less absorbing chromophores partition into the gas phase enriching aged BrC aerosol with more absorbing, non-volatile chromophores.[75,76] It is recommended that future studies systematically evaluate the effects of non-reactive volatilization and atmospheric reactive aging on BrC darkening.

3.4. Ageing of BrC chromophores from biomass burning

Transformations of BrC chromophores in BBOA during laboratory simulated atmospheric aging has been a subject of additional HPLC–PDA–HRMS studies, where stability of individual BrC species was investigated with respect to direct photolysis by UV irradiation. Fig. 12 illustrates the response of individual BrC chromophores upon photolysis under UV irradiation in the condensed phase.[106] The study determined that flavonoid and lignin-derived BrC chromophores are comparatively photoresilient. Half-lifetimes of the photolysis-sensitive chromophores vary by fuel type and burning conditions. The same BrC species can have different photolysis half-lifetimes depending on the overall BBOA composition. This variability is attributed to effects such as photosensitization, energy loss to neighboring species, and shielding by co-existing BBOA components. Interestingly, overall BrC light absorption decayed much slower (factor of 10 or more) than the photolysis of individual chromophores across all studied mixtures. This slower decay has been attributed to the formation of numerous new, lower-abundance BrC chromophores that collectively absorb in the same wavelength range, as well as the formation of high-molecular-weight, recalcitrant BrC chromophores. Different components of biofuels and burning conditions also affect the stability of BrC species. For instance, BrC in BBOA from canopy biofuel burns had longer half-lifetimes than those from non-canopy biofuels (litter and duff) burned under smoldering conditions. The long photolysis lifetimes observed for overall BrC absorption by BBOA suggest that other chemical aging processes, such as oxidation by OH and other atmospheric radicals, are likely more significant than condensed-phase photolysis for atmospheric BrC.[106]

Formation of secondary BrC chromophores from nighttime aging of BBOA by $^{\bullet}NO_3$ radicals has been observed in field studies and further tested in laboratory experiments. These experiments, using HPLC–PDA–HRMS characterization, explored the heterogeneous reactions of $^{\bullet}NO_3$ with airborne BBOA generated from pyrolysis of hardwood pellets. After $^{\bullet}NO_3$ exposure, BBOA showed significant enhancement in BrC light absorption, attributed to the formation of NAC chromophores. Fig. 13 illustrates that unreacted BBOA primarily consisted of oxygenated aromatics such as phenols with methoxy, carbonyl, and vinyl groups, whereas NAC became highly abundant after the reaction. Identified NAC species included nitrosalicylic acid, nitrophenol, nitrocatechol, dinitrophenol, and nitroguaiacol. The MAC values comparison of unreacted and reacted BBOA

 This journal is © The Royal Society of Chemistry 2025

Open Access Article. Published on 02 January 2025. Downloaded on 1/23/2026 11:08:06 PM.
This article is licensed under a Creative Commons Attribution-NonCommercial 3.0 Unported Licence.

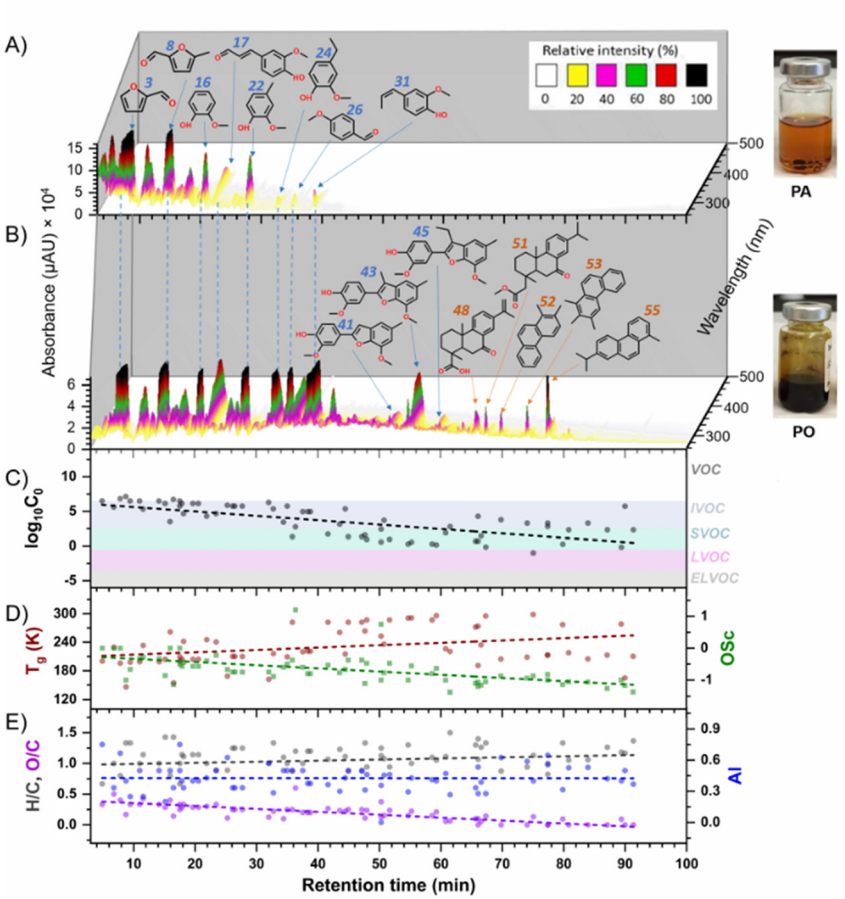

Fig. 11 Molecular properties BrC components identified in biomass pyrolysis condensates. Panels A and B present HPLC–PDA chromatograms of the 'aqueous' (PA) and 'oily' (PO) fractions. Common chromophores are highlighted in blue, while oil-specific chromophores are marked in orange. Panels C, D and E display component-specific values for volatility ($\log_{10} C_0$, μg m^{-3}), glass transition temperature (T_g, K), oxidation state (OS_C), H/C and O/C elemental ratios, and aromaticity index (AI). Background shading in panel C indicates the volatility ranges of organic compounds (OC): volatile OC (VOC), intermediate volatility (IVOC), semi-volatile (SVOC), low-volatility (LVOC) and extremely low volatility VOC (ELVOC).[167] Dashed lines represent linear trend fits. Reproduced from ref. 76 with permission from the American Chemical Society, copyright 2021.

indicated a 20–30% absorption enhancement due to the formation of NAC chromophores.

4. Characterization of BrC species in laboratory mixtures

Molecular studies of atmospheric OA composition and transformations are crucial for understanding and predicting BrC properties and their atmospheric impacts. The complexity of real-world OA composition makes it challenging to identify BrC components and their sources, as well as their aging processes in urban *versus* remote locations and during long-range transport. Targeted laboratory experiments focused on the formation and simulated aging of BrC components in OA provide valuable insights into the relationship between BrC composition and OA optical properties. The effectiveness of HPLC–PDA–HRMS for analyzing OA samples has been demonstrated in several recent studies discussed below. These studies have significantly enhanced our understanding of BrC formation and atmospheric aging, improving our ability to assess the potential effects of OA on the atmospheric environment, climate, and biogeochemical cycles.

4.1. Nitro-aromatics

Laboratory studies on the composition of SOA formed by OH-induced photooxidation of anthropogenic aromatic VOCs, such as benzene,[120] toluene[51,168–170] and naphthalene,[40,171] under different NO_x levels, have provided explicit characterization of NAC chromophores as significant BrC contributors in aged OA typical of urban areas.[172] Molecular characterization of toluene SOA formed at high NO_x conditions identified 15 major NAC products (nitro-catechols, nitro-phenols, and their derivatives) as strong BrC chromophores absorbing in the 300–500 nm UV-visible range.[51] The relative contributions of these 15 most absorbing chromophores to the overall light absorption were approximately 60% in the 300–400 nm range and around 40% in the 400–500 nm range.[51] It was concluded that NAC were the most significant secondary BrC chromophores determining the

Open Access Article. Published on 02 January 2025. Downloaded on 1/23/2026 11:08:06 PM.
This article is licensed under a Creative Commons Attribution-NonCommercial 3.0 Unported Licence.

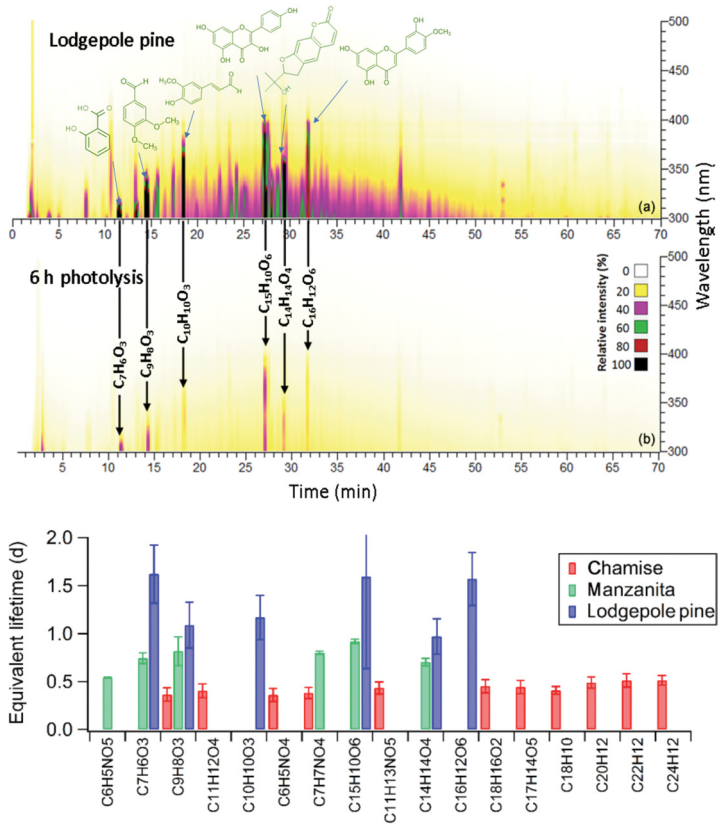

Fig. 12 HPLC–PDA chromatograms illustrating BrC species present in the BBOA sample (burning of lodgepole pine biofuel) before (a) and after (b) 300 nm irradiation. (c) Estimated atmospheric lifetimes for selected individual BrC chromophores due to UV irradiation in BBOA from different biofuels. Reproduced from ref. 106 with permission from the European Geophysical Union, copyright 2020.

optical properties of the observed SOA. Subsequent field studies corroborated that the presence of NAC in SOA formed from aromatic precursors is a common trend in urban aerosol.[172]

A systematic comparison of light absorption by SOA formed from three biogenic terpenes and eight anthropogenic aromatic precursors photo-oxidized in the presence of NO_x showed consistently higher MAC values for anthropogenic SOA, due to the formation of NAC chromophores.[120] Specifically, various isomers of methyl-nitrocatechols and related species with an added hydroxyl group were identified as the most absorbing BrC chromophores in the *m*-cresol SOA/NO_x sample, contributing to ~50% of the MAC_{365nm} value. Similarly, a few individual NAC chromophores contributed to ~30% and 20% of the MAC_{365nm} values measured for benzene SOA/NO_x and naphthalene SOA/NO_x samples, respectively. In contrast, biogenic SOA formed under the same NO_x conditions contained no NAC species and showed no BrC absorption, inherent to the non-aromatic nature of terpene precursors. Besides NAC chromophores, oxygenated hydrocarbon aromatic products also significantly contribute to the BrC absorption by anthropogenic SOA formed from polyaromatic precursors. Studies of the chemical composition and optical properties of naphthalene SOA generated with and without NO_x revealed several strongly absorbing NAC chromophores and oxygenated aromatic chromophores under both low and high NO_x conditions.[40] The majority of the BrC chromophores identified were aromatic CHO compounds with hydroxyl, carboxyl, methyl, and aldehyde functional groups, while NAC species were similar to those found in SOA generated from single-aromatic ring precursors (*e.g.*, benzene,[173] toluene,[51] cresol[120]) under high NO_x settings.[40]

4.2. Oligomers

Oligomeric species formed through multi-phase chemistry[174] in deliquesced or activated aqueous particles contribute significantly to the pool of BrC chromophores in both biogenic and anthropogenic SOA mixtures. Reactive uptake of isoprene epoxydiols (IEPOX),[175] a photochemical oxidation product of isoprene, onto wet acidic ammonium sulfate seed particles creates SOA with chemical composition and optical characteristics similar to atmospheric HULIS.[176] Chemical analysis of these SOA mixtures detected the formation of highly unsaturated oligomers composed of 5-carbon monomer units, such as $C_5H_8O_2$ and C_5H_6O, coinciding with enhanced BrC absorption. Strongly absorbing BrC species identified were oligomers of 4–8 monomer units with elemental formulas of $C_{20}H_{28}O_6$, $C_{30}H_{42}O_9$, $C_{35}H_{50}O_{11}$, and $C_{40}H_{56}O_{12}$, with respective DBE values of 7, 10, 11, and 13. Similar oligomeric products were also observed in real-world OA samples collected in rural southeast USA during summer, suggesting their atmospheric relevance.[176]

 This journal is © The Royal Society of Chemistry 2025

Open Access Article. Published on 02 January 2025. Downloaded on 1/23/2026 11:08:06 PM.
This article is licensed under a Creative Commons Attribution-NonCommercial 3.0 Unported Licence.

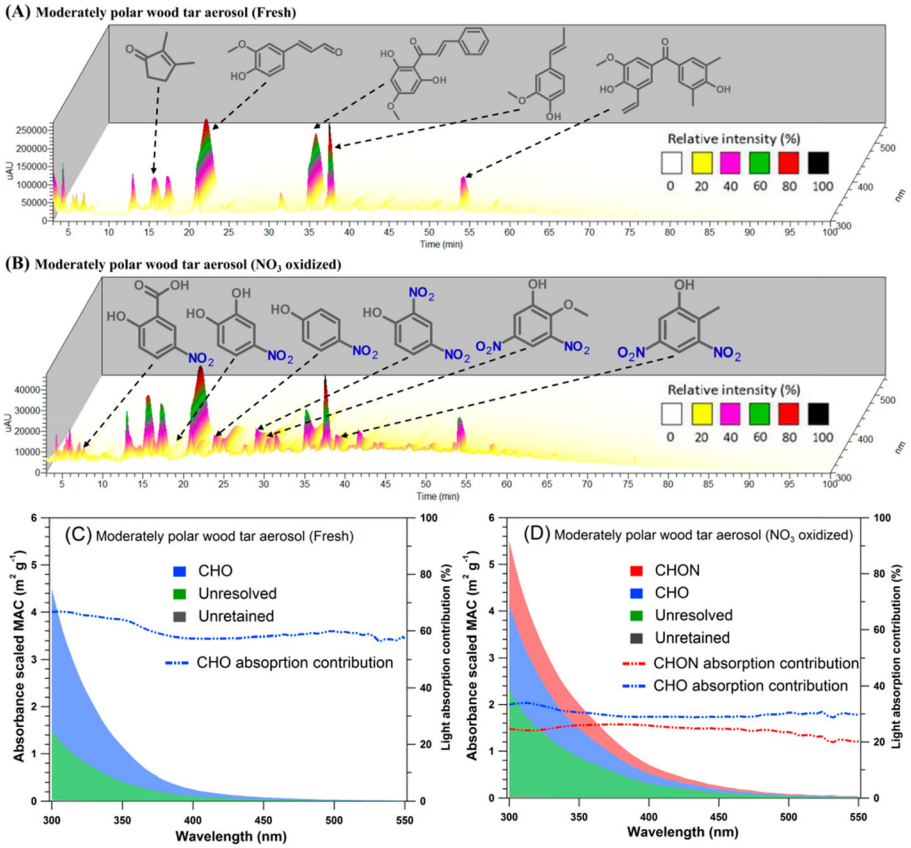

Fig. 13 Molecular characterization of fresh and $^{\bullet}NO_3$ aged BBOA prepared from hardwood pyrolysis condensate. Panels (A) and (B) show the HPLC–PDA chromatograms. Panels C and D illustrate the absorption contributions of various BrC fractions, categorized by their CHO and CHON elemental composition. Reproduced from ref. 38 with permission from the American Chemical Society, copyright 2020.

Formation of oligomeric BrC chromophores was also reported from dark aqueous-phase Fe(III)–catalyzed reactions of phenolic compounds (guaiacol, catechol, syringol, *ortho-* and *para-*cresol),[129] which are relevant in areas impacted by combined biomass burning and mineral dust emissions. Fig. 14 illustrates the results of the separation and chemical characterization of the products of guaiacol ($C_7H_8O_2$) + Fe(III) reacted mixture, highlighting UV-vis spectra and elemental formulas of the strongly absorbing BrC species.[129] The most absorbing BrC species identified were trimers ($C_{21}H_{18}O_6$ and $C_{20}H_{16}O_6$) and a tetramer ($C_{28}H_{24}O_8$), with the absorbance maxima in the visible range, around 480–490 nm. The highest extent of oligomerization was observed in the guaiacol and catechol systems, while fewer oligomers were detected in the syringol–Fe(III) mixture.[129] These differences and the molecular structures of the observed reaction products suggest that oligomers form through C–C coupling[177] of monomers at preferred *para-* and *ortho*-positions, favoring these reactions in guaiacol and catechol systems. Furthermore, no evidence of potential Fe-containing products was found in any of the four systems studied, indicating a purely catalytic role of Fe(III) under the experimental conditions employed.

4.3. Polycyclic aromatic hydrocarbons and derivatives

PAHs are common BrC species in primary exhaust emissions resulting from the incomplete combustion of hydrocarbon fuels. These emissions are often simulated in laboratory flame burners operated at fuel-rich settings and different dilution ratios with inert gases to control the composition and temperature of the emitted exhaust mixtures. Laboratory studies of BrC co-emitted with soot particles in these experiments[54,147] provide valuable information on the emission factors, OC/EC ratios, OC composition, and mass concentrations of emitted pollutants. Fig. 15a and b illustrates the separation and detection of solvent-soluble BrC species observed in aerosol samples collected from an ethane flame operated under conditions favoring OC emissions.[54] The results show a large number of BrC species with strong absorption in the ultraviolet-visible 300–500 nm wavelength range. The majority of the strong BrC chromophores are 4–7 aromatic ring PAHs and their oxygenated derivatives (O-PAH). Several of them are isomers with the same elemental formulas. Fig. 15c shows the fractions of the overall MAC values attributed to contributions from identified BrC chromophores, grouped into three operationally defined classes: semi-polar O-PAHs, nonpolar PAHs smaller and larger than benzo[*a*]pyrene (BaP). Approximately 40% of MAC is attributed to the O-PAH/quinone class, while another 40% is due to the unsubstituted PAHs. The larger $PAH_{>BaP}$ and smaller $PAH_{<BaP}$ fractions contribute approximately 20% each. The MAC values reported in that study were consistent with various field measurements of BrC generated from gasoline combustion in motor vehicles. They were also found to be 2–5 times lower than the

Open Access Article. Published on 02 January 2025. Downloaded on 1/23/2026 11:08:06 PM.
This article is licensed under a Creative Commons Attribution-NonCommercial 3.0 Unported Licence.

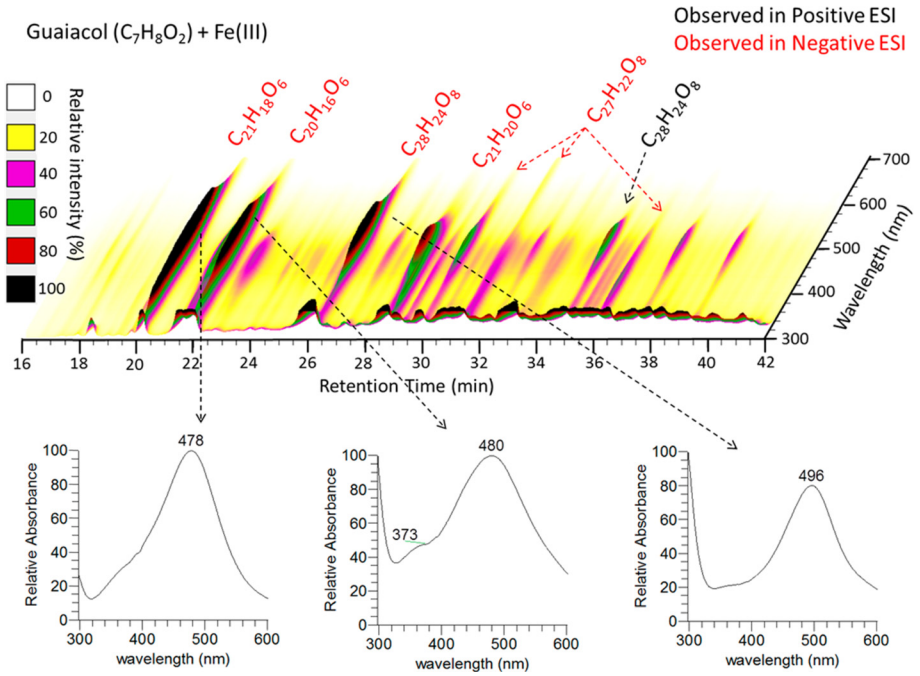

Fig. 14 HPLC–PDA chromatogram of oligomerization products in Guaiacol/Fe(III) proxies of aqueous SOA formed under dark conditions. Lower panels show UV-visible spectra of three most absorbing chromophores. Reproduced from ref. 129 with permission from the American Chemical Society, copyright 2017.

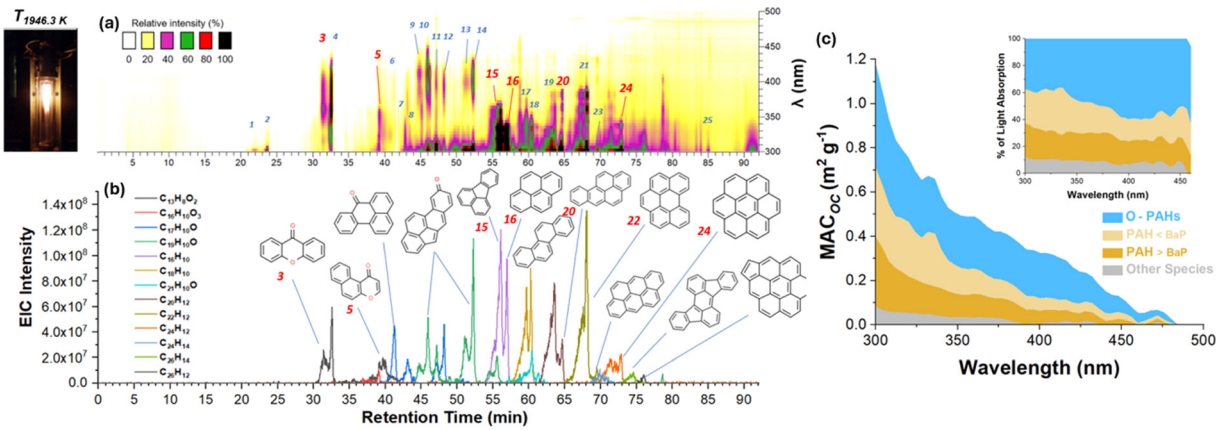

Fig. 15 HPLC–PDA (a) and HPLC–HRMS (b) chromatograms of OC extracted from aerosol sample generated by ethane flame (depicted by left insert). Experimental MAC_{OC} values fractionated with respect to relative contributions (c) of different types of chromophores: oxygenated-poly aromatic hydrocarbons (O-PAHs), PAHs smaller and larger than benzo[*a*]pyrene (BaP). Reproduced from ref. 54 with permission from the American Chemical Society, copyright 2020.

MAC values measured for typical BrC from biomass burning. Additionally, the AAE values of 4.6–6.3 measured for BrC from ethylene flames were much higher than the AAE < 2.5 commonly reported for the biomass burning BrC. These observations suggest that the stronger spectral dependence of BrC light absorption measured in field studies might be used to distinguish emissions from fossil fuel combustion *versus* biomass burning.

4.4. Reduced nitrogen containing species

BrC chromophores attributed to various oligomeric products containing moieties of primary and secondary imines (Schiff bases) were reported in many laboratory studies investigating the composition and optical properties of SOA formed in aqueous phase reactions of carbonyl-containing and reduced nitrogen (N) species (*e.g.* ammonium, imines, amines, amino acids).[52,53,99,178–185] Numerous reduced N-containing BrC species were detected in the samples collected from experiments simulating cloud cycling of ammonium- and amine-containing aerosol proxies, accompanied by the reactive uptake of gas-phase methylglyoxal (MG) and methylamine.[178] Molecular structural information about these species was further inferred from MS^n fragmentation experiments and theoretical chemistry

 This journal is © The Royal Society of Chemistry 2025

Open Access Article. Published on 02 January 2025. Downloaded on 1/23/2026 11:08:06 PM.
This article is licensed under a Creative Commons Attribution-NonCommercial 3.0 Unported Licence.

modeling of their electronic structures and corresponding UV-vis spectra. The formation of the identified BrC species was rationalized by radical addition reactions producing reduced N-containing oligomers, suggesting that sunlight can potentially enhance BrC formation under certain atmospheric conditions. Similarly, reduced N-containing chromophores were detected in the aqueous mixtures of MG and ammonium sulfate (AS), simulating formation of secondary BrC in atmospheric aerosols.[52] The identified BrC species contributed more than 70% of the overall BrC light absorption. This type of ammonium-catalyzed reaction in aqueous environments provides a unique source of imidazole and other N-heterocyclic compounds, potentially contributing to secondary BrC formed in aged SOA.

Secondary BrC chromophores formed in the di-carbonyl + amine reactions were investigated in selected atmospherically relevant mixtures of di-carbonyls (*i.e.*, glyoxal, methylglyoxal, 2,3-butanedione, 2,5-hexanedione, acetylacetone, glutaraldehyde, and acetaldehyde) reacted with ammonium sulfate and glycine in pH ranges from 1.7 to 4.9.[53] Fig. 16 illustrates the HPLC–PDA heatmaps and integrated spectral range chromatograms of the aqueous acetaldehyde + acetylacetone/ammonium sulfate mixture analyzed after 0.5 h and 144 h of reaction time. The major BrC chromophore, eluted at ~8 min, corresponds to the ion $C_{12}H_{18}O_2N^+$ attributed to a six-membered ring nitrogen heterocyclic compound inferred from the tandem MS^2 fragmentation experiments. This BrC species exhibits a strong absorption feature at ~380 nm, responsible for the bulk BrC absorption in the acetaldehyde + acetylacetone/ammonium sulfate system. Additional N-heterocyclic/aromatic imidazoles, pyrroles, (dihydro-)pyridines, and di-pyrromethenes in the other di-carbonyl + amine reaction pools were observed as secondary BrC chromophores formed in the experimental mixtures.[53] The specific BrC products differ for each reacting system and may potentially undergo additional photochemical aging under solar UV-vis light. Reduced N-containing BrC chromophores were also detected in limonene SOA aged in the presence of either ammonia or glycine amino acid, forming monomeric, dimeric, trimeric, and tetrameric BrC species containing imine (−CH═NH) and Schiff base (−CH═N−R) moieties.[99,183–185] These N-containing species strongly absorb UV-visible light in the 400–600 nm range, characteristic of secondary BrC materials.

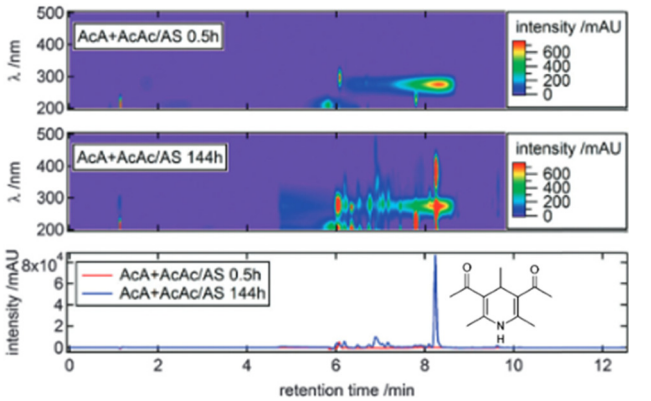

Fig. 16 HPLC–PDA heatmaps for acetaldehyde + acetylacetone/ammonium sulfate at 0.5 h (top) and 144 h (middle) of reaction time. PDA chromatograms integrated over the 300–500 nm wavelength range retrieved from the two above records. The assigned structure of BrC species eluted at 8.3 min is shown in bottom panel, representing the neutral formula, $C_{12}H_{17}O_2N$. Reproduced from ref. 53 with permission from the Royal Chemical Society, copyright 2016.

N-Containing heterocycles compounds are also naturally occurring biogenic VOCs emitted from animal husbandry and variety of plants. Laboratory studies on the photochemical oxidation of indole, a representative species of this type, have shown that the resulting SOA is visibly colored and exhibits distinctive absorption bands in the visible spectrum.[56,186] The major BrC species separated and identified in these experiments corresponded to indole derivatives such as tryptanthrin, indirubin, indigo dye, and indoxyl red, all significantly contributing to the observed BrC light absorption.[186] The role of indole as a significant secondary BrC precursor potentially emitted from stressed plants under oxidative atmospheric conditions was demonstrated by the results from these studies.

4.5. Colloidal BrC components

Recent studies indicate that an important yet often overlooked type of BrC species in atmospheric mixtures are insoluble colloids formed from iron-catalyzed aqueous reactions of common biomass burning emission components such as catechol, nitrocatechols, and water-soluble carboxylic acids.[121,187–189] Research on the dark Fe(III)–catalyzed reactions of catechol reports the formation of insoluble black polycatechol particles and water-soluble BrC species under conditions representative of viscous multicomponent aerosol systems with high ionic strength and acidic pH.[189] The soluble BrC species were identified as substituted monoaromatic compounds and quinones, while aggregated insoluble polycatechol colloids were detected *via* dynamic light scattering. The polycatechol colloidal particles were observed in solutions of variable ionic strength, containing selected carboxylic acids undergoing dark reactions in the presence of dissolved Fe(III). The rate of colloid growth and agglomeration was highest for solutions of Fe(III)/catechol and ammonium sulfate under low ionic strength and slower for Fe(III)/catechol systems containing competing carboxylate ligands and higher ionic strength. Follow-up research using additional mixtures of various nitrophenols[187] and replicas of BBOA complex mixtures[188] corroborated earlier observations, confirming that colloidal BrC species can be produced from dark iron-catalyzed reactions in aging aerosol plumes across a wide range of aerosol physical states and chemical compositions.

The photochemical generation and growth of BrC colloidal particles from irradiated Fe(III)–citrate aqueous mixtures, a relevant laboratory proxy for Fe(III)–carboxylate complexes in atmospheric aerosols, have also been reported.[121] Analysis of the reaction products identified water-soluble Fe(III)–citrate complexes, intermediate Fe(II)–organic complexes, and water-soluble organic acids and oligomeric products. Prolonged

Open Access Article. Published on 02 January 2025. Downloaded on 1/23/2026 11:08:06 PM.
This article is licensed under a Creative Commons Attribution-NonCommercial 3.0 Unported Licence.

irradiation led to a systematic decrease in the BrC absorbance of soluble species, with the remaining absorbance attributed to carbonaceous colloids that formed and grew in size. These BrC colloids were identified as unsaturated organic species with low oxygen content and a reduced oxidation state.

Therefore, the formation of insoluble colloidal material driven by iron chemistry under both dark and light conditions is a potentially important source of colloidal BrC in the atmospheric environment. It should be noted that colloids cannot be directly analyzed *via* HPLC–PDA–HRMS without proper sample digestion and relevant sample preparation. The current analytical chemistry methods for colloidal BrC analysis are inadequate, necessitating the development of novel analytical measurements for suspended colloidal materials in atmospheric chemistry.

4.6. Effects of atmospheric aging

The composition and properties of atmospheric OA undergo constant evolution due to a combination of chemical and physical aging processes, such as direct photolysis, multiphase reactions, gas-particle partitioning, water uptake, phase separations, *etc.*[43,190,191] During daytime, OA ageing is dominated by photolysis and reactions with $^{\bullet}OH$, while nighttime ageing is mostly governed by reactions with $^{\bullet}NO_3$ and O_3, although daytime reactions with O_3 can also be significant.[43,62,102,106,107,192–197] Throughout their diurnal pattern, oxidants modify OA, altering their role in atmospheric chemistry and radiative forcing. Daytime reactions with $^{\bullet}OH$ (in absence of NO_x or SO_2) degrade OA chromophores and decrease BrC absorption.[43,62,102,106,192,193,195,198] In contrast, nighttime reactions of $^{\bullet}NO_3$ form new nitro-aromatic chromophores that enhance the BrC absorption.[33,107,196,199–201]

Diversity in the chemical composition of OA mixtures and their BrC species has an intrinsic impact on their ageing transformations under the same oxidation conditions. Photochemical degradation of various BrC components varies substantially, with smaller species yielding more volatile degradation products capable of gas-phase partitioning. Larger BrC species are not only more resistant to photochemical degradation, but their decomposition products can still be large enough to retain BrC properties and remain in the condensed phase.[102,106] Similarly, while the formation of the relatively small light absorbing nitro-phenols has been reported in experiments with freshly formed OA,[33,51,107] the impact of the same nighttime chemistry on aged OA is yet unknown. Additionally, photoexcitation of larger aromatic BrC chromophores in OA can promote the corresponding molecules to their highly reactive triplet excited states ($^3C^*$),[202,203] which can either directly react with other OA molecules through electron-transfer reactions[204–206] or induce the formation of other strong oxidants, such as singlet molecular oxygen[207,208] and hydrogen peroxide.[208]

Transformations of OA are also influenced by the non-reactive gas-particle partitioning of its individual species. The loss of small monoaromatic compounds in biomass burning OA leads to the accumulation of larger lignin decomposition fragments, substantially enhancing BrC absorption.[75,76] Simultaneously, the volatility and viscosity of the aged OA mixtures evolve, preserving less volatile and more viscous constituents, consequently augmenting the overall BrC absorbance of the OA mixtures.[75] Advancing the predictive understanding of real-world OA transformations requires considering multiple aging pathways. Therefore, systematic studies of sequential nighttime and daytime reactive chemistry, together with the effects of gas-particle partitioning, are needed to improve the phenomenological understanding of BrC transformations and to guide modeling developments.

5. Integrating molecular composition of BrC into modeling frameworks

Advances in the studies of BrC molecular composition, optical properties, sources, and aging transformations have yielded critical experimental data that now inform modern modeling approaches. These efforts integrate BrC chemistry with climate science and data analysis science to develop advanced predictive modeling frameworks. Recent progress has focused on two primary fronts: (1) the development of machine learning models to accurately link BrC molecular composition to its optical characteristics[87–93] and (2) the simulation of regional variability and atmospheric impacts of BrC across different geographic regions.[94–97] This section highlights key findings from recent advancements in both areas.

5.1. Predictions of BrC optical properties from molecular composition

Machine learning (ML) approaches provide powerful tools for modeling the complex relationships between BrC's molecular composition and its optical properties. A notable study employed a random forest ML algorithm to quantify the contributions of different atmospheric HULIS sources to measurable bulk BrC optical parameters such as MAC(λ) and AAE.[91] Another investigation utilized random forest models to identify molecular markers of atmospheric BrC from HRMS data, revealing that 17 nitrogen-containing species effectively characterized BrC absorption variability.[93] More recently, an explainable random forest model was applied to correlate the mass concentrations and light absorption of four common groups of BrC chromophores (16 PAHs, 9 O-PAHs, 11 NACs, and 2 methoxyphenols – MOPs) with the optical properties of methanol-soluble bulk BrC extracts.[88] To further clarify the relationships between BrC's optical properties and its chemical composition, the study employed the Shapley Additive Explanation (SHAP) method, providing insights into how individual chromophores contribute to BrC's optical behavior.[88] Fig. 17 illustrates results from this work, highlighting the ML modeling ability to accurately reproduce temporal variations in BrC absorbance and mass absorption coefficients, demonstrating its strong predictive performance.

A key challenge in predicting BrC optical properties using ML approaches lies in the need for extensive, high-quality

 This journal is © The Royal Society of Chemistry 2025

Open Access Article. Published on 02 January 2025. Downloaded on 1/23/2026 11:08:06 PM.
This article is licensed under a Creative Commons Attribution-NonCommercial 3.0 Unported Licence.

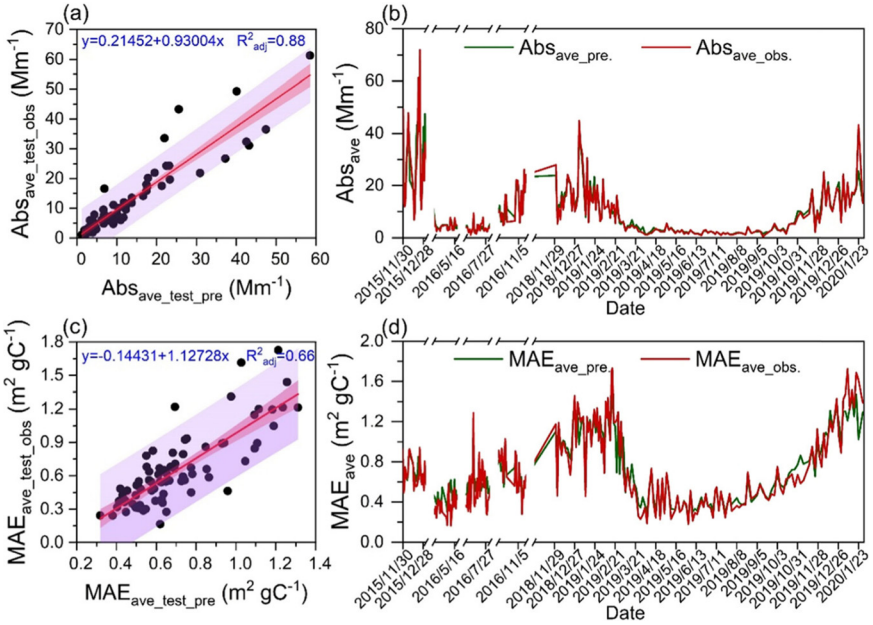

Fig. 17 (a) and (b) Random forest model performance for the test dataset, showing predicted *versus* observed average BrC absorbance (Abs_{ave_pre} and Abs_{ave_obs}) integrated over the 300–500 nm wavelength range, along with time-resolved records; (c) and (d) Corresponding data sets presented as mass absorption coefficients (or efficiency, MAE_{save_pre} and MAE_{ave_obs}, as labeled in these plots), demonstrating close agreement between predicted and observed values. Reproduced from ref. 88 with permission from the American Chemical Society, copyright 2024.

training datasets that adequately represent the molecular diversity of BrC. This is further complicated by the diverse sources of BrC and the complex interactions between its molecular structures and light, which can lead to considerable uncertainties in predictions. Additionally, ML models often face difficulties when applied to data that diverge from the conditions or features present in the training datasets. Another critical issue is the limited interpretability of ML results, as advancing scientific understanding of BrC requires uncovering the physicochemical mechanisms underlying model predictions rather than relying solely on statistical outputs. Despite these challenges, recent advancements in molecular characterization, as highlighted in this review, have begun to establish detailed molecular profiles of BrC. These profiles serve as valuable training datasets for ML models but are derived from highly specialized and resource-intensive HRMS instrumentation. Such analyses are both labor-intensive and costly, presenting barriers to adoption in research groups lacking expertise in this technology. However, as ML models continue to improve in accuracy and generalization, their predictive capabilities are expected to reduce the reliance on extensive HRMS measurements. Eventually, these models may offer cost-effective and time-efficient alternatives for estimating BrC optical properties across various atmospheric environments. The integration of ML techniques into BrC research offers a promising path forward, enabling predictions of optical properties from basic molecular descriptors. Although meaningful progress in ML applications for BrC research has been recently demonstrated,[87–93] overcoming challenges related to data variability, model generalization, and interpretability remains essential for driving further advancements in this field.

5.2. Composition-driven insights into the regional variability and optical behavior of atmospheric BrC.

Although global models have incorporated BrC absorption,[14–22] their reliance on simplified assumptions about emission sources, chemical composition, and optical properties, coupled with limited understanding of BrC atmospheric transformations, continues to introduce uncertainties. Similarly, efforts to model BrC's impact on regional air quality, visibility, and climate forcing remain underdeveloped. Recent advancements in molecular characterization have significantly improved understanding of BrC sources and properties, enabling better modeling of its optical behavior, temporal dynamics, and interactions with other atmospheric components. These developments began to inform chemical transport regional models, improving their ability to evaluate BrC environmental and climatic impacts.[94–97] For example, a recent study integrated prognostic modifications of BrC optical properties into a three-dimensional chemical transport model, focusing on biomass burning emissions.[96] BrC was represented as a mixture of three components: inert – iBrC, reactive – rBrC, and photobleached – phBrC. The iBrC was treated as persistent condensed-phase species with very low volatility ($c^* < 10^{-2}$ μg m^{-3}), while rBrC and phBrC components followed the broader volatility distribution of BBOA ($10^{-2} < c^* < 10^{6}$ μg m^{-3}), allowing for gas-phase partitioning and reactions. The imaginary refractive indices at 550 nm were set to 0.044 for iBrC and rBrC and 0.008 for phBrC. The model also incorporated a photobleaching reaction converting rBrC into phBrC, based on first-order kinetics derived from laboratory studies.[195] Fig. 18 illustrates results from that work displaying calculated impact of BrC on

Open Access Article. Published on 02 January 2025. Downloaded on 1/23/2026 11:08:06 PM.
This article is licensed under a Creative Commons Attribution-NonCommercial 3.0 Unported Licence.

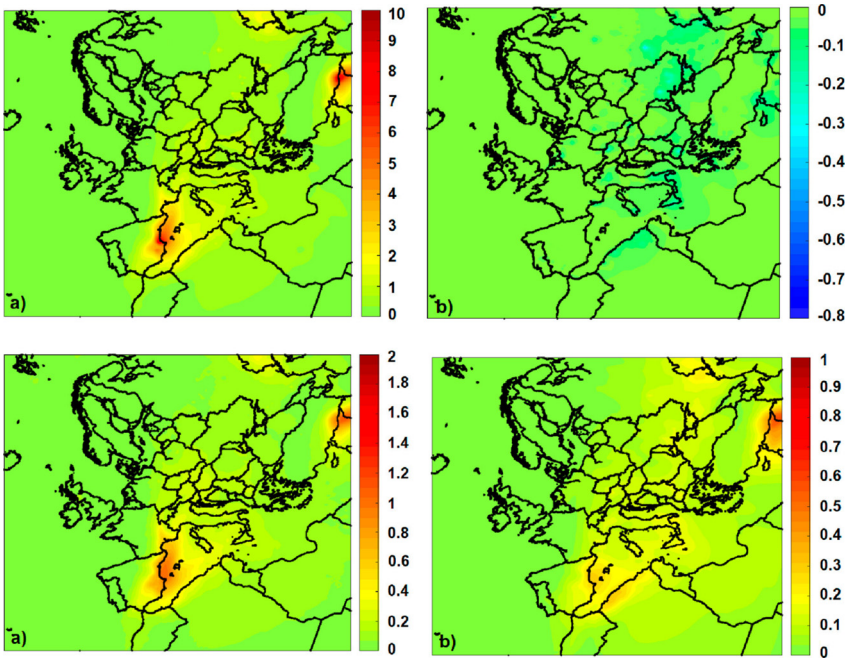

Fig. 18 Upper panel: Modeled average % contribution of BrC to (a) aerosol optical depth (AOD) and (b) single scattering albedo (SSA) at 550 nm. Lower panel: Modeled average % impact of BrC photobleaching on (a) AOD and (b) SSA at 550 nm. Reproduced from ref. 96 with permission from the American Chemical Society, copyright 2024.

aerosol optical depth (AOD) and single scattering albedo (SSA) over Europe averaged for the simulation time period. Upper panel plots show that overall BrC causes a 10% increase in AOD near major fire events and around 5–6% in areas 800–1000 km downwind, while its effect on SSA is marginal, mostly lower than 0.3%. As BrC undergoes photobleaching it becomes less absorbing, which modifies AOD and SSA. Lower panel plots decipher the explicit effects of BrC photobleaching on the aerosol optical properties which causes an increase in both AOD and SSA due to the increase of phBrC fractions. Along with other recent studies, this work introduced one of the first prognostic implementations of BrC in chemical transport models, incorporating variability in composition, properties, and transformation processes.[94–97] Performance of these models was evaluated by comparing simulated outputs with observational data retrieved from the AErosol RObotic NETwork (AERONET) and MODIS satellite platforms.[94–97] These studies underscored substantial influence of BrC over large regions across all continents, particularly in areas where surface BrC concentrations have surged due to the increased frequency of wildfires driven by a warming climate, alongside rising anthropogenic emissions linked to population growth and industrial activity. These modeling advancements pave the way for a more comprehensive exploration of BrC prognostic impacts on atmospheric processes and environmental systems.

6. Summary and future outlook

The molecular characterization of BrC components in OA mixtures has yielded significant scientific insights into a diverse range of atmospheric light-absorbing species. These studies have enabled the differentiation of various BrC types and sources, such as those primarily emitted from biomass burning and those formed through secondary reactions in multi-phase atmospheric chemistry. Notably, the discovery of compounds like nitro-aromatics, polyphenols, and quinones, which play key roles in BrC's optical properties, was made possible through this detailed analysis. The formation pathways of BrC have also been elucidated, particularly in identifying relevant atmospheric reactions, including those involving reduced nitrogen species, phenolic compounds, and iron-catalyzed processes. Additionally, these studies have provided unique insights into the chemical aging of BrC, demonstrating how its composition and optical properties evolve over time due to photolysis, oxidation, and other atmospheric processes. This includes the degradation of chromophores and the formation of new light-absorbing species under varying environmental conditions. Furthermore, a direct correlation between BrC molecular composition and its UV-vis light absorption has been established, crucial for accurately modeling its impact on atmospheric radiative forcing. The high sensitivity and versatility of HRMS characterization have led to the discovery of previously unknown BrC species, significantly expanding the understanding of the diversity and complexity of OA components in the atmosphere. Overall, molecular analysis using the HPLC–PDA–HRMS platform has provided a comprehensive and detailed understanding of BrC, advancing knowledge of its chemical makeup, formation processes, and environmental impact in ways that were not possible with earlier analytical techniques.

 This journal is © The Royal Society of Chemistry 2025

Open Access Article. Published on 02 January 2025. Downloaded on 1/23/2026 11:08:06 PM.
This article is licensed under a Creative Commons Attribution-NonCommercial 3.0 Unported Licence.

Future research on the molecular characterization of atmospheric BrC should focus on several key areas. The application of ultra-high-resolution mass spectrometry (UHRMS) techniques will be essential for better detection and identification of additional BrC components, such as those containing sulfur and phosphorus compounds, as well as for assessing isotopic patterns. Incorporating ion mobility spectrometry (IMS) into the HPLC–PDA–HRMS chemical characterization framework could offer deeper insights into the structural composition of BrC species and their isomers. Further efforts should be made to discover and characterize new BrC precursor molecules, particularly those from biogenic sources, anthropogenic activities, and biomass burning. Exploring the contributions of lesser-known sources, including marine aerosols, agricultural emissions, and urban environments, will broaden the understanding of BrC atmospheric significance. Detailed studies on the chemical aging processes of BrC, such as photochemical oxidation and interactions with atmospheric oxidants, are needed to clarify how BrC species evolve over time. Investigating the role of multiphase reactions in cloud and fog droplets, as well as in aqueous aerosol particles, in BrC formation and evolution under different environmental conditions, will also be crucial. Future research should aim to characterize the molecular structure, optical properties, and environmental behavior of colloidal BrC formed from iron-catalyzed reactions and other pathways. Understanding the formation and growth of these colloids can shed light on their role in atmospheric light absorption and radiative forcing. Improved analytical methods are necessary to detect and characterize colloidal BrC in environmental samples, including the development of novel techniques for sampling, digestion, and analysis. Given the time- and labor-intensive nature of experimental characterization of BrC chromophores, modern computational tools employing artificial intelligence and machine learning should be developed. These tools should focus on predicting quantitative BrC properties from LC-HRMS datasets, streamlining the research process and accelerating advancements in the field.

Quantifying the radiative effects of BrC, including its interactions with clouds, is essential. Improving atmospheric and climate models to reflect BrC diverse chemical composition and optical properties will enhance predictions of its environmental impact. Additionally, research on BrC health effects of BrC, especially its role in respiratory and cardiovascular diseases, is also vital. Field studies conducted in various environments, coupled with controlled laboratory experiments, will bridge the gap between real-world emissions and laboratory findings. Promoting interdisciplinary collaboration among atmospheric chemists, climate scientists, toxicologists, and policymakers will foster a holistic understanding of BrC and its implications for the atmospheric environment, health, and climate. Developing more accurate predictive models to forecast BrC formation, evolution, and transport in the atmosphere is also critical. These models should incorporate the latest findings on BrC chemistry, aging processes, and interactions with other atmospheric constituents. Expanding studies to assess the global and regional impacts of BrC on climate and air quality, including long-range transport and deposition, will enhance the understanding of its environmental significance. Addressing these research directions will advance the molecular characterization of BrC and improve strategies for managing air quality and climate.

Data availability

No primary research results, software or codes have been included and no new data were generated or analyzed as part of this review.

Conflicts of interest

There are no conflicts to declare.

Acknowledgements

We gratefully acknowledge funding from the U.S. National Science Foundation, Grants AGS-2039985 and CHE-2404150, for research support at the time of this manuscript compilation. Additional support for past research projects of our group described in this review has been provided by the U.S. Department of Commerce and National Oceanic and Atmospheric Administration, Climate Program Office's AC4 program; the U.S. Department of Energy, Office of Biological and Environmental Research (BER) through Atmospheric System Research program and through sponsorship of the William R. Wiley Environmental Molecular Sciences Laboratory.

References

1 M. O. Andreae and A. Gelencsér, Black carbon or brown carbon? The nature of light-absorbing carbonaceous aerosols, *Atmos. Chem. Phys.*, 2006, **6**(10), 3131–3148.
2 A. Laskin, J. Laskin and S. A. Nizkorodov, Chemistry of Atmospheric Brown Carbon, *Chem. Rev.*, 2015, **115**(10), 4335–4382.
3 T. Moise, J. M. Flores and Y. Rudich, Optical Properties of Secondary Organic Aerosols and Their Changes by Chemical Processes, *Chem. Rev.*, 2015, **115**(10), 4400–4439.
4 R. Bahadur, P. S. Praveen, Y. Y. Xu and V. Ramanathan, Solar absorption by elemental and brown carbon determined from spectral observations, *Proc. Natl. Acad. Sci. U. S. A.*, 2012, **109**(43), 17366–17371.
5 Y. Z. Zhang, H. Forrister, J. M. Liu, J. Dibb, B. Anderson, J. P. Schwarz, A. E. Perring, J. L. Jimenez, P. Campuzano-Jost, Y. H. Wang, A. Nenes and R. J. Weber, Top-of-atmosphere radiative forcing affected by brown carbon in the upper troposphere, *Nat. Geosci.*, 2017, **10**(7), 486–489.
6 C. H. Xie, W. Q. Xu, J. F. Wang, Q. Q. Wang, D. T. Liu, G. Q. Tang, P. Chen, W. Du, J. Zhao, Y. J. Zhang, W. Zhou, T. T. Han, Q. Y. Bian, J. Li, P. Q. Fu, Z. F. Wang, X. L. Ge, J. Allan, H. Coe and Y. L. Sun, Vertical characterization of aerosol optical properties and brown carbon in winter in

Open Access Article. Published on 02 January 2025. Downloaded on 1/23/2026 11:08:06 PM. This article is licensed under a Creative Commons Attribution-NonCommercial 3.0 Unported Licence.

urban Beijing, China, *Atmos. Chem. Phys.*, 2019, **19**(1), 165–179.

7 S. Bikkina and M. Sarin, Brown carbon in the continental outflow to the North Indian Ocean, *Environ. Sci.: Processes Impacts*, 2019, **21**(6), 970–987.

8 Q. Wang, Y. Han, J. Ye, S. Liu, S. Pongpiachan, N. Zhang, Y. Han, J. Tian, C. Wu, X. Long, Q. Zhang, W. Zhang, Z. Zhao and J. Cao, High Contribution of Secondary Brown Carbon to Aerosol Light Absorption in the Southeastern Margin of Tibetan Plateau, *Geophys. Res. Lett.*, 2019, **46**(9), 4962–4970.

9 N. Evangeliou, A. Kylling, S. Eckhardt, V. Myroniuk, K. Stebel, R. Paugam, S. Zibtsev and A. Stohl, Open fires in Greenland in summer 2017: transport, deposition and radiative effects of BC, OC and BrC emissions, *Atmos. Chem. Phys.*, 2019, **19**(2), 1393–1411.

10 X. Wang, H. Wei, J. Liu, B. Xu, M. Wang, M. Ji and H. Jin, Quantifying the light absorption and source attribution of insoluble light-absorbing particles on Tibetan Plateau glaciers between 2013 and 2015, *The Cryosphere*, 2019, **13**(1), 309–324.

11 C. D. Cappa, X. L. Zhang, L. M. Russell, S. Collier, A. K. Y. Lee, C. L. Chen, R. Betha, S. J. Chen, J. Liu, D. J. Price, K. J. Sanchez, G. R. McMeeking, L. R. Williams, T. B. Onasch, D. R. Worsnop, J. Abbatt and Q. Zhang, Light Absorption by Ambient Black and Brown Carbon and its Dependence on Black Carbon Coating State for Two California, USA, Cities in Winter and Summer, *J. Geophys. Res.: Atmos.*, 2019, **124**(3), 1550–1577.

12 A. X. Zhang, Y. H. Wang, Y. Z. Zhang, R. J. Weber, Y. J. Song, Z. M. Ke and Y. F. Zou, Modeling the global radiative effect of brown carbon: a potentially larger heating source in the tropical free troposphere than black carbon, *Atmos. Chem. Phys.*, 2020, **20**(4), 1901–1920.

13 A. Pandey, A. Hsu, S. Tiwari, S. Pervez and R. K. Chakrabarty, Light Absorption by Organic Aerosol Emissions Rivals That of Black Carbon from Residential Biomass Fuels in South Asia, *Environ. Sci. Technol. Lett.*, 2020, **7**(4), 266–272.

14 Y. Feng, V. Ramanathan and V. R. Kotamarthi, Brown carbon: a significant atmospheric absorber of solar radiation?, *Atmos. Chem. Phys.*, 2013, **13**(17), 8607–8621.

15 X. Wang, C. L. Heald, D. A. Ridley, J. P. Schwarz, J. R. Spackman, A. E. Perring, H. Coe, D. Liu and A. D. Clarke, Exploiting simultaneous observational constraints on mass and absorption to estimate the global direct radiative forcing of black carbon and brown carbon, *Atmos. Chem. Phys.*, 2014, **14**(20), 10989–11010.

16 M. Z. Jacobson, Effects of biomass burning on climate, accounting for heat and moisture fluxes, black and brown carbon, and cloud absorption effects, *J. Geophys. Res.: Atmos.*, 2014, **119**(14), 8980–9002.

17 G. X. Lin, J. E. Penner, M. G. Flanner, S. Sillman, L. Xu and C. Zhou, Radiative forcing of organic aerosol in the atmosphere and on snow: effects of SOA and brown carbon, *J. Geophys. Res.: Atmos.*, 2014, **119**(12), 7453–7476.

18 R. Saleh, M. Marks, J. Heo, P. J. Adams, N. M. Donahue and A. L. Robinson, Contribution of brown carbon and lensing to the direct radiative effect of carbonaceous aerosols from biomass and biofuel burning emissions, *J. Geophys. Res.: Atmos.*, 2015, **120**(19), 10285–10296.

19 M. S. Hammer, R. V. Martin, A. van Donkelaar, V. Buchard, O. Torres, D. A. Ridley and R. J. D. Spurr, Interpreting the ultraviolet aerosol index observed with the OMI satellite instrument to understand absorption by organic aerosols: implications for atmospheric oxidation and direct radiative effects, *Atmos. Chem. Phys.*, 2016, **16**(4), 2507–2523.

20 D. S. Jo, R. J. Park, S. Lee, S. W. Kim and X. L. Zhang, A global simulation of brown carbon: implications for photochemistry and direct radiative effect, *Atmos. Chem. Phys.*, 2016, **16**(5), 3413–3432.

21 H. Brown, X. H. Liu, Y. Feng, Y. Q. Jiang, M. X. Wu, Z. Lu, C. L. Wu, S. Murphy and R. Pokhrel, Radiative effect and climate impacts of brown carbon with the Community Atmosphere Model (CAM5), *Atmos. Chem. Phys.*, 2018, **18**(24), 17745–17768.

22 X. Wang, C. L. Heald, J. M. Liu, R. J. Weber, P. Campuzano-Jost, J. L. Jimenez, J. P. Schwarz and A. E. Perring, Exploring the observational constraints on the simulation of brown carbon, *Atmos. Chem. Phys.*, 2018, **18**(2), 635–653.

23 M. R. Olson, A. Lai, M. Skiles and J. J. Schauer, Attribution of Source Specific 370 nm UV Light Absorption from Dust, Brown Carbon, and Black Carbon at Two Locations in the San Joaquin Valley, *Aerosol Air Qual. Res.*, 2024, **24**(4), 230292.

24 S. Liu, T. Luo, L. Zhou, T. Song, N. Wang, Q. Luo, G. Huang, X. Jiang, S. Zhou, Y. Qiu and F. Yang, Vehicle exhausts contribute high near-UV absorption through carbonaceous aerosol during winter in a fast-growing city of Sichuan Basin, China, *Environ. Pollut.*, 2022, **312**, 119966.

25 N. Y. Kasthuriarachchi, L. H. Rivellini, M. G. Adam and A. K. Y. Lee, Light Absorbing Properties of Primary and Secondary Brown Carbon in a Tropical Urban Environment, *Environ. Sci. Technol.*, 2020, **54**(17), 10808–10819.

26 M. Zhang, D. Cai, J. Lin, Z. Liu, M. Li, Y. Wang and J. Chen, Molecular characterization of atmospheric organic aerosols in typical megacities in China, *npj Clim. Atmos. Sci.*, 2024, **7**(1), 230.

27 C. Yan, M. Zheng, C. Bosch, A. Andersson, Y. Desyaterik, A. P. Sullivan, J. L. Collett, B. Zhao, S. Wang, K. He and Ö. Gustafsson, Important fossil source contribution to brown carbon in Beijing during winter, *Sci. Rep.*, 2017, **7**(1), 43182.

28 H. Ni, R.-J. Huang, S. M. Pieber, J. C. Corbin, G. Stefenelli, V. Pospisilova, F. Klein, M. Gysel-Beer, L. Yang, U. Baltensperger, I. E. Haddad, J. G. Slowik, J. Cao, A. S. H. Prévôt and U. Dusek, Brown Carbon in Primary and Aged Coal Combustion Emission, *Environ. Sci. Technol.*, 2021, **55**(9), 5701–5710.

29 R. Saleh, C. J. Hennigan, G. R. McMeeking, W. K. Chuang, E. S. Robinson, H. Coe, N. M. Donahue and A. L. Robinson, Absorptivity of brown carbon in fresh and photo-chemically

 This journal is © The Royal Society of Chemistry 2025

Open Access Article. Published on 02 January 2025. Downloaded on 1/23/2026 11:08:06 PM. This article is licensed under a Creative Commons Attribution-NonCommercial 3.0 Unported Licence.

aged biomass-burning emissions, *Atmos. Chem. Phys.*, 2013, **13**(15), 7683–7693.

30 N. K. Kumar, J. C. Corbin, E. A. Bruns, D. Massabó, J. G. Slowik, L. Drinovec, G. Močnik, P. Prati, A. Vlachou, U. Baltensperger, M. Gysel, I. El-Haddad and A. S. H. Prévôt, Production of particulate brown carbon during atmospheric aging of residential wood-burning emissions, *Atmos. Chem. Phys.*, 2018, **18**(24), 17843–17861.

31 A. T. Ahern, E. S. Robinson, D. S. Tkacik, R. Saleh, L. E. Hatch, K. C. Barsanti, C. E. Stockwell, R. J. Yokelson, A. A. Presto, A. L. Robinson, R. C. Sullivan and N. M. Donahue, Production of Secondary Organic Aerosol During Aging of Biomass Burning Smoke From Fresh Fuels and Its Relationship to VOC Precursors, *J. Geophys. Res.: Atmos.*, 2019, **124**(6), 3583–3606.

32 C. Sarkar, C. Venkataraman, S. Yadav, H. C. Phuleria and A. Chatterjee, Origin and properties of soluble brown carbon in freshly emitted and aged ambient aerosols over an urban site in India, *Environ. Pollut.*, 2019, **254**(Part B), 113077.

33 C. Li, Q. He, J. Schade, J. Passig, R. Zimmermann, D. Meidan, A. Laskin and Y. Rudich, Dynamic changes in optical and chemical properties of tar ball aerosols by atmospheric photochemical aging, *Atmos. Chem. Phys.*, 2019, **19**(1), 139–163.

34 X. J. Fan, T. Cao, X. F. Yu, Y. Wang, X. Xiao, F. Y. Li, Y. Xie, W. C. Ji, J. Z. Song and P. A. Peng, The evolutionary behavior of chromophoric brown carbon during ozone aging of fine particles from biomass burning, *Atmos. Chem. Phys.*, 2020, **20**(8), 4593–4605.

35 X. R. Li, Y. Yang, S. Q. Liu, Q. Zhao, G. H. Wang and Y. S. Wang, Light absorption properties of brown carbon (BrC) in autumn and winter in Beijing: composition, formation and contribution of nitrated aromatic compounds, *Atmos. Environ.*, 2020, **223**, 117289.

36 C. Peng, M. Tian, X. L. Wang, F. M. Yang, G. M. Shi, R. J. Huang, X. J. Yao, Q. Y. Wang, C. Z. Zhai, S. M. Zhang, R. Z. Qian, J. J. Cao and Y. Chen, Light absorption of brown carbon in $PM_{2.5}$ in the Three Gorges Reservoir region, southwestern China: implications of biomass burning and secondary formation, *Atmos. Environ.*, 2020, **229**, 117409.

37 K. Vidovic, A. Kroflic, M. Sala and I. Grgic, Aqueous-Phase Brown Carbon Formation from Aromatic Precursors under Sunlight Conditions, *Atmosphere*, 2020, **11**(2), 131.

38 C. Li, Q. He, A. P. S. Hettiyadura, U. Käfer, G. Shmul, D. Meidan, R. Zimmermann, S. S. Brown, C. George, A. Laskin and Y. Rudich, Formation of Secondary Brown Carbon in Biomass Burning Aerosol Proxies through NO_3 Radical Reactions, *Environ. Sci. Technol.*, 2020, **54**(3), 1395–1405.

39 C. Li, Q. He, Z. Fang, S. S. Brown, A. Laskin, S. R. Cohen and Y. Rudich, Laboratory Insights into the Diel Cycle of Optical and Chemical Transformations of Biomass Burning Brown Carbon Aerosols, *Environ. Sci. Technol.*, 2020, **54**(19), 11827–11837.

40 K. Siemens, A. Morales, Q. F. He, C. L. Li, A. P. S. Hettiyadura, Y. Rudich and A. Laskin, Molecular Analysis of Secondary Brown Carbon Produced from the Photooxidation of Naphthalene, *Environ. Sci. Technol.*, 2022, **56**(6), 3340–3353.

41 J. Yan, X. Wang, P. Gong, C. Wang and Z. Cong, Review of brown carbon aerosols: recent progress and perspectives, *Sci. Total Environ.*, 2018, **634**, 1475–1485.

42 Y. J. Wang, M. Hu, X. Li and N. Xu, Chemical Composition, Sources and Formation Mechanisms of Particulate Brown Carbon in the Atmosphere, *Prog. Chem.*, 2020, **32**(5), 627–641.

43 R. F. Hems, E. G. Schnitzler, C. Liu-Kang, C. D. Cappa and J. P. D. Abbatt, Aging of Atmospheric Brown Carbon Aerosol, *ACS Earth Space Chem.*, 2021, **5**(4), 722–748.

44 Q. Wang, Y. Zhou, N. Ma, Y. Zhu, X. Zhao, S. Zhu, J. Tao, J. Hong, W. Wu, Y. Cheng and H. Su, Review of Brown Carbon Aerosols in China: Pollution Level, Optical Properties, and Emissions, *J. Geophys. Res.: Atmos.*, 2022, **127**(16), e2021JD035473.

45 R. Saleh, From Measurements to Models: Toward Accurate Representation of Brown Carbon in Climate Calculations, *Curr. Pollut. Rep.*, 2020, **6**, 90–104.

46 M. Zhong and M. Jang, Light absorption coefficient measurement of SOA using a UV-Visible spectrometer connected with an integrating sphere, *Atmos. Environ.*, 2011, **45**(25), 4263–4271.

47 K. M. Updyke, T. B. Nguyen and S. A. Nizkorodov, Formation of brown carbon via reactions of ammonia with secondary organic aerosols from biogenic and anthropogenic precursors, *Atmos. Environ.*, 2012, **63**, 22–31.

48 J. M. Flores, R. A. Washenfelder, G. Adler, H. J. Lee, L. Segev, J. Laskin, A. Laskin, S. A. Nizkorodov, S. S. Brown and Y. Rudich, Complex refractive indices in the near-ultraviolet spectral region of biogenic secondary organic aerosol aged with ammonia, *Phys. Chem. Chem. Phys.*, 2014, **16**(22), 10629–10642.

49 J. M. Flores, D. F. Zhao, L. Segev, P. Schlag, A. Kiendler-Scharr, H. Fuchs, A. K. Watne, N. Bluvshtein, T. F. Mentel, M. Hallquist and Y. Rudich, Evolution of the complex refractive index in the UV spectral region in ageing secondary organic aerosol, *Atmos. Chem. Phys.*, 2014, **14**(11), 5793–5806.

50 P. F. Liu, N. Abdelmalki, H. M. Hung, Y. Wang, W. H. Brune and S. T. Martin, Ultraviolet and visible complex refractive indices of secondary organic material produced by photooxidation of the aromatic compounds toluene and m-Xylene, *Atmos. Chem. Phys. Discuss.*, 2014, **14**(14), 20585–20615.

51 P. Lin, J. Liu, J. E. Shilling, S. M. Kathmann, J. Laskin and A. Laskin, Molecular Characterization of Brown Carbon (BrC) Chromophores in Secondary Organic Aerosol Generated From Photo-Oxidation of Toluene, *Phys. Chem. Chem. Phys.*, 2015, **17**, 23312–23325.

52 P. Lin, J. Laskin, S. A. Nizkorodov and A. Laskin, Revealing Brown Carbon Chromophores Produced in Reactions of Methylglyoxal with Ammonium Sulfate, *Environ. Sci. Technol.*, 2015, **49**(24), 14257–14266.

Open Access Article. Published on 02 January 2025. Downloaded on 1/23/2026 11:08:06 PM. This article is licensed under a Creative Commons Attribution-NonCommercial 3.0 Unported Licence.

53 C. J. Kampf, A. Filippi, C. Zuth, T. Hoffmann and T. Opatz, Secondary brown carbon formation via the dicarbonyl imine pathway: nitrogen heterocycle formation and synergistic effects, *Phys. Chem. Chem. Phys.*, 2016, **18**(27), 18353–18364.

54 C. P. West, A. P. S. Hettiyadura, A. Darmody, G. Mahamuni, J. Davis, I. Novosselov and A. Laskin, Molecular Composition and the Optical Properties of Brown Carbon Generated by the Ethane Flame, *ACS Earth Space Chem.*, 2020, **4**(7), 1090–1103.

55 N. G. Jimenez, K. D. Sharp, T. Gramyk, D. Z. Ugland, M. K. Tran, A. Rojas, M. A. Rafla, D. Stewart, M. M. Galloway, P. Lin, A. Laskin, M. Cazaunau, E. Pangui, J. F. Doussin and D. O. De Haan, Radical-Initiated Brown Carbon Formation in Sunlit Carbonyl-Amine-Ammonium Sulfate Mixtures and Aqueous Aerosol Particles, *ACS Earth Space Chem.*, 2021, **6**(1), 228–238.

56 F. Jiang, K. Siemens, C. Linke, Y. Li, Y. Gong, T. Leisner, A. Laskin and H. Saathoff, Molecular analysis of secondary organic aerosol and brown carbon from the oxidation of indole, *Atmos. Chem. Phys.*, 2024, **24**(4), 2639–2649.

57 P. Lin, P. K. Aiona, Y. Li, M. Shiraiwa, J. Laskin, S. A. Nizkorodov and A. Laskin, Molecular Characterization of Brown Carbon in Biomass Burning Aerosol Particles, *Environ. Sci. Technol.*, 2016, **50**(21), 11815–11824.

58 P. Lin, N. Bluvshtein, Y. Rudich, S. A. Nizkorodov, J. Laskin and A. Laskin, Molecular Chemistry of Atmospheric Brown Carbon Inferred from a Nationwide Biomass Burning Event, *Environ. Sci. Technol.*, 2017, **51**(20), 11561–11570.

59 P. Lin, L. T. Fleming, S. A. Nizkorodov, J. Laskin and A. Laskin, Comprehensive Molecular Characterization of Atmospheric Brown Carbon by High Resolution Mass Spectrometry with Electrospray and Atmospheric Pressure Photoionization, *Anal. Chem.*, 2018, **90**(21), 12493–12502.

60 J. Xu, A. P. S. Hettiyadura, Y. Liu, X. Zhang, S. Kang and A. Laskin, Regional Differences of Chemical Composition and Optical Properties of Aerosols in the Tibetan Plateau, *J. Geophys. Res.: Atmos.*, 2020, **125**(1), e2019JD031226.

61 J. Z. Xu, A. P. S. Hettiyadura, Y. M. Liu, X. H. Zhang, S. C. Kang and A. Laskin, Atmospheric Brown Carbon on the Tibetan Plateau: Regional Differences in Chemical Composition and Light Absorption Properties, *Environ. Sci. Technol. Lett.*, 2022, **9**(3), 219–225.

62 E. C. Browne, X. L. Zhang, J. P. Franklin, K. J. Ridley, T. W. Kirchstetter, K. R. Wilson, C. D. Cappa and J. H. Kroll, Effect of heterogeneous oxidative aging on light absorption by biomass burning organic aerosol, *Aerosol Sci. Technol.*, 2019, **53**(6), 663–674.

63 D. Sengupta, V. Samburova, C. Bhattarai, E. Kirillova, L. Mazzoleni, M. Iaukea-Lum, A. Watts, H. Moosmüller and A. Khlystov, Light absorption by polar and non-polar aerosol compounds from laboratory biomass combustion, *Atmos. Chem. Phys.*, 2018, **18**, 10849–10867.

64 P. Tiitta, A. Leskinen, L. Q. Hao, P. Yli-Pirila, M. Kortelainen, J. Grigonyte, J. Tissari, H. Lamberg, A. Hartikainen, K. Kuuspalo, A. M. Kortelainen, A. Virtanen, K. E. J. Lehtinen, M. Komppula, S. Pieber, A. S. H. Prevot, T. B. Onasch, D. R. Worsnop, H. Czech, R. Zimmermann, J. Jokiniemi and O. Sippula, Transformation of logwood combustion emissions in a smog chamber: formation of secondary organic aerosol and changes in the primary organic aerosol upon daytime and nighttime aging, *Atmos. Chem. Phys.*, 2016, **16**(20), 13251–13269.

65 J. Saturno, B. A. Holanda, C. Pöhlker, F. Ditas, Q. Wang, D. Moran-Zuloaga, J. Brito, S. Carbone, Y. Cheng, X. Chi, J. Ditas, T. Hoffmann, I. Hrabe de Angelis, T. Könemann, J. V. Lavrič, N. Ma, J. Ming, H. Paulsen, M. L. Pöhlker, L. V. Rizzo, P. Schlag, H. Su, D. Walter, S. Wolff, Y. Zhang, P. Artaxo, U. Pöschl and M. O. Andreae, Black and brown carbon over central Amazonia: long-term aerosol measurements at the ATTO site, *Atmos. Chem. Phys.*, 2018, **18**(17), 12817–12843.

66 K. Siemens, T. Paik, A. Li, F. Rivera-Adorno, J. Tomlin, Q. Xie, R. K. Chakrabarty and A. Laskin, Light Absorption and Chemical Composition of Brown Carbon Organic Aerosol Produced from Burning of Selected Biofuels, *ACS Earth Space Chem.*, 2024, **8**(7), 1416–1428.

67 K. Adachi, A. J. Sedlacek, L. Kleinman, S. R. Springston, J. Wang, D. Chand, J. M. Hubbe, J. E. Shilling, T. B. Onasch, T. Kinase, K. Sakata, Y. Takahashi and P. R. Buseck, Spherical tarball particles form through rapid chemical and physical changes of organic matter in biomass-burning smoke, *Proc. Natl. Acad. Sci. U. S. A.*, 2019, **116**(39), 19336–19341.

68 D. T. L. Alexander, P. A. Crozier and J. R. Anderson, Brown carbon spheres in East Asian outflow and their optical properties, *Science*, 2008, **321**(5890), 833–836.

69 A. J. Sedlacek Iii, P. R. Buseck, K. Adachi, T. B. Onasch, S. R. Springston and L. Kleinman, Formation and evolution of tar balls from northwestern US wildfires, *Atmos. Chem. Phys.*, 2018, **18**(15), 11289–11301.

70 D. P. Veghte, S. China, J. Weis, L. Kovarik, M. K. Gilles and A. Laskin, Optical Properties of Airborne Soil Organic Particles, *ACS Earth Space Chem.*, 2017, **1**(8), 511–521.

71 J. Laskin, A. Laskin and S. A. Nizkorodov, Mass Spectrometry Analysis in Atmospheric Chemistry, *Anal. Chem.*, 2018, **90**(1), 166–189.

72 H. X. Jiang, J. Li, J. Tang, Y. Z. Mo and G. Zhang, Applications of High-Resolution Mass Spectrometry in Studies of Brown Carbon, *Chin. J. Anal. Chem.*, 2018, **46**(10), 1528–1537.

73 F. A. Houle, A. A. Wiegel and K. R. Wilson, Predicting Aerosol Reactivity Across Scales: from the Laboratory to the Atmosphere, *Environ. Sci. Technol.*, 2018, **52**(23), 13774–13781.

74 S. Papazian, L. A. D'Agostino, I. Sadiktsis, J. Froment, B. Bonnefille, K. Sdougkou, H. Xie, I. Athanassiadis, K. Budhavant, S. Dasari, A. Andersson, Ö. Gustafsson and J. W. Martin, Nontarget mass spectrometry and in silico molecular characterization of air pollution from the Indian subcontinent, *Commun. Earth Environ.*, 2022, **3**(1), 35.

75 D. Calderon-Arrieta, A. C. Morales, A. P. S. Hettiyadura, T. M. Estock, C. Li, Y. Rudich and A. Laskin, Enhanced Light Absorption and Elevated Viscosity of Atmospheric

 This journal is © The Royal Society of Chemistry 2025

Open Access Article. Published on 02 January 2025. Downloaded on 1/23/2026 11:08:06 PM. This article is licensed under a Creative Commons Attribution-NonCommercial 3.0 Unported Licence.

Brown Carbon through Evaporation of Volatile Components, *Environ. Sci. Technol.*, 2024, **58**(17), 7493–7504.

76 A. P. S. Hettiyadura, V. Garcia, C. L. Li, C. P. West, J. Tomlin, Q. F. He, Y. Rudich and A. Laskin, Chemical Composition and Molecular-Specific Optical Properties of Atmospheric Brown Carbon Associated with Biomass Burning, *Environ. Sci. Technol.*, 2021, **55**(4), 2511–2521.

77 Y. Zhou, C. P. West, A. P. S. Hettiyadura, W. Pu, T. L. Shi, X. Y. Niu, H. Wen, J. C. Cui, X. Wang and A. Laskin, Molecular Characterization of Water-Soluble Brown Carbon Chromophores in Snowpack from Northern Xinjiang, China, *Environ. Sci. Technol.*, 2022, **56**(7), 4173–4186.

78 D. Cai, C. Li, J. Lin, W. Sun, M. Zhang, T. Wang, M. Abudumutailifu, Y. Lyu, X. Huang, X. Li and J. Chen, Comparative study of atmospheric brown carbon at Shanghai and the East China Sea: Molecular characterization and optical properties, *Sci. Total Environ.*, 2024, **941**, 173782.

79 V. Moschos, C. Christensen, M. Mouton, M. N. Fiddler, T. Isolabella, F. Mazzei, D. Massabò, B. J. Turpin, S. Bililign and J. D. Surratt, Quantifying the Light-Absorption Properties and Molecular Composition of Brown Carbon Aerosol from Sub-Saharan African Biomass Combustion, *Environ. Sci. Technol.*, 2024, **58**(9), 4268–4280.

80 A. P. S. Hettiyadura and A. Laskin, Quantitative analysis of polycyclic aromatic hydrocarbons using high-performance liquid chromatography-photodiode array-high-resolution mass spectrometric detection platform coupled to electrospray and atmospheric pressure photoionization sources, *J. Mass Spectrom.*, 2022, **57**(2), e4804.

81 S. Hildmann and T. Hoffmann, Characterisation of atmospheric organic aerosols with one- and multidimensional liquid chromatography and mass spectrometry: state of the art and future perspectives, *TrAC, Trends Anal. Chem.*, 2024, **175**, 117698.

82 A. K. Alang and S. G. Aggarwal, Atmospheric Brown Carbon: Sources, Optical Properties, and Chromophore Composition, *Aerosol Air Qual. Res.*, 2024, **24**(9), 240035.

83 W. Yuan, R. J. Huang, L. Yang, J. Guo, Z. Chen, J. Duan, T. Wang, H. Ni, Y. Han, Y. Li, Q. Chen, Y. Chen, T. Hoffmann and C. O'Dowd, Characterization of the light-absorbing properties, chromophore composition and sources of brown carbon aerosol in Xi'an, northwestern China, *Atmos. Chem. Phys.*, 2020, **20**(8), 5129–5144.

84 R.-J. Huang, L. Yang, J. Cao, Y. Chen, Q. Chen, Y. Li, J. Duan, C. Zhu, W. Dai, K. Wang, C. Lin, H. Ni, J. C. Corbin, Y. Wu, R. Zhang, X. Tie, T. Hoffmann, C. O'Dowd and U. Dusek, Brown Carbon Aerosol in Urban Xi'an, Northwest China: The Composition and Light Absorption Properties, *Environ. Sci. Technol.*, 2018, **52**(12), 6825–6833.

85 C. Yan, M. Zheng, Y. Desyaterik, A. P. Sullivan, Y. Wu and J. L. Collett Jr., Molecular Characterization of Water-Soluble Brown Carbon Chromophores in Beijing, China, *J. Geophys. Res.: Atmos.*, 2020, **125**(15), e2019JD032018.

86 X. Wang, N. Hayeck, M. Brüggemann, L. Abis, M. Riva, Y. Lu, B. Wang, J. Chen, C. George and L. Wang, Chemical Characteristics and Brown Carbon Chromophores of Atmospheric Organic Aerosols Over the Yangtze River Channel: A Cruise Campaign, *J. Geophys. Res.: Atmos.*, 2020, **125**(16), e2020JD032497.

87 E. Tapavicza, G. F. von Rudorff, D. O. De Haan, M. Contin, C. George, M. Riva and O. A. von Lilienfeld, Elucidating an Atmospheric Brown Carbon Species—Toward Supplanting Chemical Intuition with Exhaustive Enumeration and Machine Learning, *Environ. Sci. Technol.*, 2021, **55**(12), 8447–8457.

88 Y. Wang, R.-J. Huang, H. Zhong, T. Wang, L. Yang, W. Yuan, W. Xu and Z. An, Predictions of the Optical Properties of Brown Carbon Aerosol by Machine Learning with Typical Chromophores, *Environ. Sci. Technol.*, 2024, **58**(46), 20588–20597.

89 A. Zhang, Y. Zeng, X. Yang, J. Zhai, Y. Wang, C. Xing, B. Cai, S. Shi, Y. Zhang, Z. Shen, T.-M. Fu, L. Zhu, H. Shen, J. Ye and C. Wang, Organic Matrix Effect on the Molecular Light Absorption of Brown Carbon, *Geophys. Res. Lett.*, 2023, **50**(24), e2023GL106541.

90 Y. Huang, X. Li, D. D. Huang, R. Lei, B. Zhou, Y. Zhang and X. Ge, Machine Learning Assisted Chemical Characterization and Optical Properties of Atmospheric Brown Carbon in Nanjing, China, *EGUsphere*, 2024, **2024**, 1–66.

91 Y. Hong, F. Cao, M.-Y. Fan, Y.-C. Lin, M. Bao, Y. Xue, J. Wu, M. Yu, X. Wu and Y.-L. Zhang, Using machine learning to quantify sources of light-absorbing water-soluble humic-like substances (HULISws) in Northeast China, *Atmos. Environ.*, 2022, **291**, 119371.

92 Z. Guo, W. Sun, X. Hu, J. Lin, Y. Fu, X. Peng, B. Jiang, Y. Liao, G. Zhang, X. Wang, P. A. Peng and X. Bi, Molecular characteristics and compositions affecting light absorption features of cloud water revealed by Fourier transform ion cyclotron resonance mass spectrometry, *Atmos. Environ.*, 2023, **295**, 119565.

93 H. Jiang, J. Li, R. Sun, C. Tian, J. Tang, B. Jiang, Y. Liao, C.-E. Chen and G. Zhang, Molecular Dynamics and Light Absorption Properties of Atmospheric Dissolved Organic Matter, *Environ. Sci. Technol.*, 2021, **55**(15), 10268–10279.

94 L. Xu, G. Lin, X. Liu, C. Wu, Y. Wu and S. Lou, Constraining Light Absorption of Brown Carbon in China and Implications for Aerosol Direct Radiative Effect, *Geophys. Res. Lett.*, 2024, **51**(16), e2024GL109861.

95 F. Wang, Z. Lu, G. Lin, G. R. Carmichael and M. Gao, Brown Carbon in East Asia: Seasonality, Sources, and Influences on Regional Climate and Air Quality, *ACS Environ. Au*, 2024, DOI: **10.1021/acsenvironau.4c00080**.

96 K. Skyllakou, M.-B. Korras-Carraca, C. Matsoukas, N. Hatzianastassiou, S. N. Pandis and A. Nenes, Predicted Concentrations and Optical Properties of Brown Carbon from Biomass Burning over Europe, *ACS ES&T Air*, 2024, **1**(8), 897–908.

97 M. A. DeLessio, K. Tsigaridis, S. E. Bauer, J. Chowdhary and G. L. Schuster, Modeling atmospheric brown carbon in the GISS ModelE Earth system model, *Atmos. Chem. Phys.*, 2024, **24**(10), 6275–6304.

98 T. Letzel, E. Rosenberg, R. Wissiack, M. Grasserbauer and R. Niessner, Separation and identification of polar degradation

Open Access Article. Published on 02 January 2025. Downloaded on 1/23/2026 11:08:06 PM. This article is licensed under a Creative Commons Attribution-NonCommercial 3.0 Unported Licence.

products of benzo[a]pyrene with ozone by atmospheric pressure chemical ionization-mass spectrometry after optimized column chromatographic clean-up, *J. Chromatogr. A*, 1999, **855**(2), 501–514.

99 T. B. Nguyen, A. Laskin, J. Laskin and S. A. Nizkorodov, Brown carbon formation from ketoaldehydes of biogenic monoterpenes, *Faraday Discuss.*, 2013, **165**, 473–494.

100 J. Laskin, A. Laskin, S. A. Nizkorodov, P. J. Roach, P. Eckert, M. K. Gilles, B. Wang, J. Lee and Q. Hu, Molecular Selectivity of Brown Carbon Chromophores, *Environ. Sci. Technol.*, 2014, **48**(20), 12047–12055.

101 K. S. Hopstock, A. L. Klodt, Q. R. Xie, M. A. Alvarado, A. Laskin and S. A. Nizkorodov, Photolytic aging of organic aerosol from pyrolyzed urban materials, *Environ. Sci.: Atmos.*, 2023, **3**, 1272–1285.

102 H. J. J. Lee, P. K. Aiona, A. Laskin, J. Laskin and S. A. Nizkorodov, Effect of solar radiation on the optical properties and molecular composition of laboratory proxies of atmospheric brown carbon, *Environ. Sci. Technol.*, 2014, **48**(17), 10217–10226.

103 Z. Krivácsy, A. Gelencsér, G. Kiss, E. Mészáros, Á. Molnár, A. Hoffer, T. Mészáros, Z. Sárvári, D. Temesi, B. Varga, U. Baltensperger, S. Nyeki and E. Weingartner, Study on the Chemical Character of Water Soluble Organic Compounds in Fine Atmospheric Aerosol at the Jungfraujoch, *J. Atmos. Chem.*, 2001, **39**(3), 235–259.

104 S. H. Budisulistiorini, M. Riva, M. Williams, J. Chen, M. Itoh, J. D. Surratt and M. Kuwata, Light-Absorbing Brown Carbon Aerosol Constituents from Combustion of Indonesian Peat and Biomass, *Environ. Sci. Technol.*, 2017, **51**(8), 4415–4423.

105 M. Claeys, R. Vermeylen, F. Yasmeen, Y. Gomez-Gonzalez, X. G. Chi, W. Maenhaut, T. Meszaros and I. Salma, Chemical characterisation of humic-like substances from urban, rural and tropical biomass burning environments using liquid chromatography with UV/vis photodiode array detection and electrospray ionisation mass spectrometry, *Environ. Chem.*, 2012, **9**(3), 273–284.

106 L. T. Fleming, P. Lin, J. M. Roberts, V. Selimovic, R. Yokelson, J. Laskin, A. Laskin and S. A. Nizkorodov, Molecular composition and photochemical lifetimes of brown carbon chromophores in biomass burning organic aerosol, *Atmos. Chem. Phys.*, 2020, **20**(2), 1105–1129.

107 C. L. Li, Q. F. He, A. P. S. Hettiyadura, U. Kafer, G. Shmul, D. Meidan, R. Zimmermann, S. S. Brown, C. George, A. Laskin and Y. Rudich, Formation of Secondary Brown Carbon in Biomass Burning Aerosol Proxies through NO_3 Radical Reactions, *Environ. Sci. Technol.*, 2020, **54**(3), 1395–1405.

108 Y.-H. Lin, S. H. Budisulistiorini, K. Chu, R. A. Siejack, H. Zhang, M. Riva, Z. Zhang, A. Gold, K. E. Kautzman and J. D. Surratt, Light-absorbing oligomer formation in secondary organic aerosol from reactive uptake of isoprene epoxydiols, *Environ. Sci. Technol.*, 2014, **48**(20), 12012–12021.

109 L. T. Fleming, P. Lin, A. Laskin, J. Laskin, R. Weltman, R. D. Edwards, N. K. Arora, A. Yadav, S. Meinardi, D. R. Blake, A. Pillarisetti, K. R. Smith and S. A. Nizkorodov, Molecular composition of particulate matter emissions from dung and brushwood burning household cookstoves in Haryana, India, *Atmos. Chem. Phys.*, 2018, **18**(4), 2461–2480.

110 R.-J. Huang, L. Yang, J. Shen, W. Yuan, Y. Gong, J. Guo, W. Cao, J. Duan, H. Ni, C. Zhu, W. Dai, Y. Li, Y. Chen, Q. Chen, Y. Wu, R. Zhang, U. Dusek, C. O'Dowd and T. Hoffmann, Water-Insoluble Organics Dominate Brown Carbon in Wintertime Urban Aerosol of China: Chemical Characteristics and Optical Properties, *Environ. Sci. Technol.*, 2020, **54**(13), 7836–7847.

111 Y. Chen and T. C. Bond, Light absorption by organic carbon from wood combustion, *Atmos. Chem. Phys.*, 2010, **10**(4), 1773–1787.

112 Y. Cheng, K.-b He, Z.-y Du, G. Engling, J.-m Liu, Y.-l Ma, M. Zheng and R. J. Weber, The characteristics of brown carbon aerosol during winter in Beijing, *Atmos. Environ.*, 2016, **127**, 355–364.

113 Y. Desyaterik, Y. Sun, X. Shen, T. Lee, X. Wang, T. Wang and J. L. Collett, Jr., Speciation of "brown" carbon in cloud water impacted by agricultural biomass burning in eastern China, *J. Geophys. Res.: Atmos.*, 2013, **118**(13), 7389–7399.

114 B. B. Demoz, J. L. Collett and B. C. Daube, On the Caltech Active Strand Cloudwater Collectors, *Atmos. Res.*, 1996, **41**(1), 47–62.

115 Y. Cai, Y. e Cai, Y. Shi, J. Liu, S. Mou and Y. Lu, A liquid–liquid extraction technique for phthalate esters with water-soluble organic solvents by adding inorganic salts, *Microchim. Acta*, 2007, **157**(1), 73–79.

116 D. Tomasini, F. Cacciola, F. Rigano, D. Sciarrone, P. Donato, M. Beccaria, E. B. Caramão, P. Dugo and L. Mondello, Complementary analytical liquid chromatography methods for the characterization of aqueous phase from pyrolysis of lignocellulosic biomasses, *Anal. Chem.*, 2014, **86**(22), 11255–11262.

117 H. B. Guo, F. He, B. H. Gu, L. Y. Liang and J. C. Smith, Time-Dependent Density Functional Theory Assessment of UV Absorption of Benzoic Acid Derivatives, *J. Phys. Chem. A*, 2012, **116**(48), 11870–11879.

118 H. O. T. Pye, A. Nenes, B. Alexander, A. P. Ault, M. C. Barth, S. L. Clegg, J. L. Collett, K. M. Fahey, C. J. Hennigan, H. Herrmann, M. Kanakidou, J. T. Kelly, I. T. Ku, V. F. McNeill, N. Riemer, T. Schaefer, G. L. Shi, A. Tilgner, J. T. Walker, T. Wang, R. Weber, J. Xing, R. A. Zaveri and A. Zuend, The acidity of atmospheric particles and clouds, *Atmos. Chem. Phys.*, 2020, **20**(8), 4809–4888.

119 X. Zhang, Y.-H. Lin, J. D. Surratt and R. J. Weber, Sources, Composition and Absorption Angstrom Exponent of Light-absorbing Organic Components in Aerosol Extracts from the Los Angeles Basin, *Environ. Sci. Technol.*, 2013, **47**(8), 3685–3693.

120 M. Xie, X. Chen, M. D. Hays, M. Lewandowski, J. Offenberg, T. E. Kleindienst and A. L. Holder, Light Absorption of Secondary Organic Aerosol: Composition and Contribution of Nitroaromatic Compounds, *Environ. Sci. Technol.*, 2017, **51**(20), 11607–11616.

 This journal is © The Royal Society of Chemistry 2025

Open Access Article. Published on 02 January 2025. Downloaded on 1/23/2026 11:08:06 PM. This article is licensed under a Creative Commons Attribution-NonCommercial 3.0 Unported Licence.

121 C. P. West, A. C. Morales, J. Ryan, M. V. Misovich, A. P. S. Hettiyadura, F. Rivera-Adorno, J. M. Tomlin, A. Darmody, B. N. Linn, P. Lin and A. Laskin, Molecular investigation of the multi-phase photochemistry of Fe(III)–citrate in aqueous solution, *Environ. Sci.: Processes Impacts*, 2023, **25**(2), 190–213.

122 K. S. A. Siemens, D. Pagonis, H. Guo, P. Campuzano-Jost, J.-L. Jimenez and A. Laskin, Probing Atmospheric Aerosol by Multi-modal Mass Spectrometry Techniques: Revealing Aging Characteristics of its Individual Molecular Components, *ACS Earth Space Chem.*, 2023, **7**(12), 2498–2510.

123 S. M. Phillips and G. D. Smith, Light Absorption by Charge Transfer Complexes in Brown Carbon Aerosols, *Environ. Sci. Technol. Lett.*, 2014, **1**, 382–386.

124 T. Spranger, D. van Pinxteren and H. Herrmann, Two-Dimensional Offline Chromatographic Fractionation for the Characterization of Humic-Like Substances in Atmospheric Aerosol Particles, *Environ. Sci. Technol.*, 2017, **51**(9), 5061–5070.

125 A. Laskin, P. Lin, J. Laskin, L. T. Fleming and S. Nizkorodov, Molecular Characterization of Atmospheric Brown Carbon, in *Multiphase Environmental Chemistry in the Atmosphere*, ed. S. W. Hunt, A. Laskin and S. A. Nizkorodov, 2018, vol. 1299, pp. 261–274.

126 Y. Zhou, C. P. West, D. Calderon–Arrieta, M. Misovich, A. P. S. Hettiyadura, T. Shi, J. Cui, H. Wen, W. Pu, X. Wang and A. Laskin, Photolytic Degradation of Water–Soluble Organic Carbon from Ambient Snow: Changes in Molecular Characteristics, Composition of Brown Carbon Chromophores, and Radiative Effects, *J. Geophys. Res.: Atmos.*, 2024, **129**, e2024JD040755.

127 Y. Zhou, C. P. West, A. P. S. Hettiyadura, X. Niu, H. Wen, J. Cui, T. Shi, W. Pu, X. Wang and A. Laskin, Measurement report: molecular composition, optical properties, and radiative effects of water-soluble organic carbon in snowpack samples from northern Xinjiang, China, *Atmos. Chem. Phys.*, 2021, **21**(11), 8531–8555.

128 M. V. Misovich, A. P. S. Hettiyadura, W. Jiang, Q. Zhang and A. Laskin, Molecular-Level Study of the Photo-Oxidation of Aqueous-Phase Guaiacyl Acetone in the Presence of 3C*: Formation of Brown Carbon Products, *ACS Earth Space Chem.*, 2021, **5**(8), 1983–1996.

129 A. Lavi, P. Lin, B. Bhaduri, R. Carmieli, A. Laskin and Y. Rudich, Characterization of Light-Absorbing Oligomers from Phenolic Compounds and Fe(III), *ACS Earth Space Chem.*, 2017, **1**(10), 637–646.

130 T. B. Nguyen, K. H. Bates, J. D. Crounse, R. H. Schwantes, X. Zhang, H. G. Kjaergaard, J. D. Surratt, P. Lin, A. Laskin, J. H. Seinfeld and P. O. Wennberg, Mechanism of the hydroxyl radical oxidation of methacryloyl peroxynitrate (MPAN) and its pathway toward secondary organic aerosol formation in the atmosphere, *Phys. Chem. Chem. Phys.*, 2015, **17**(27), 17914–17926.

131 Z. Kitanovski, A. Čusak, I. Grgić and M. Claeys, Chemical characterization of the main products formed through aqueous-phase photonitration of guaiacol, *Atmos. Meas. Tech.*, 2014, **7**(8), 2457–2470.

132 D. B. Robb and M. W. Blades, State-of-the-art in atmospheric pressure photoionization for LC/MS, *Anal. Chim. Acta*, 2008, **627**(1), 34–49.

133 L. C. Short, S.-S. Cai and J. A. Syage, APPI-MS: Effects of mobile phases and VUV lamps on the detection of PAH compounds, *J. Am. Soc. Mass Spectrom.*, 2007, **18**(4), 589–599.

134 W. C. Hockaday, J. M. Purcell, A. G. Marshall, J. A. Baldock and P. G. Hatcher, Electrospray and photoionization mass spectrometry for the characterization of organic matter in natural waters: a qualitative assessment, *Limnol. Oceanogr.: Methods*, 2009, **7**(1), 81–95.

135 T. Pluskal, S. Castillo, A. Villar-Briones and M. Orešič, MZmine 2: Modular framework for processing, visualizing, and analyzing mass spectrometry-based molecular profile data, *BMC Bioinf.*, 2010, **11**(1), 395.

136 R. Schmid, S. Heuckeroth, A. Korf, A. Smirnov, O. Myers, T. S. Dyrlund, R. Bushuiev, K. J. Murray, N. Hoffmann, M. Lu, A. Sarvepalli, Z. Zhang, M. Fleischauer, K. Dührkop, M. Wesner, S. J. Hoogstra, E. Rudt, O. Mokshyna, C. Brungs, K. Ponomarov, L. Mutabdžija, T. Damiani, C. J. Pudney, M. Earll, P. O. Helmer, T. R. Fallon, T. Schulze, A. Rivas-Ubach, A. Bilbao, H. Richter, L.-F. Nothias, M. Wang, M. Orešič, J.-K. Weng, S. Böcker, A. Jeibmann, H. Hayen, U. Karst, P. C. Dorrestein, D. Petras, X. Du and T. Pluskal, Integrative analysis of multimodal mass spectrometry data in MZmine 3, *Nat. Biotechnol.*, 2023, **41**(4), 447–449.

137 C. A. Smith, E. J. Want, G. O'Maille, R. Abagyan and G. Siuzdak, XCMS: Processing Mass Spectrometry Data for Metabolite Profiling Using Nonlinear Peak Alignment, Matching, and Identification, *Anal. Chem.*, 2006, **78**(3), 779–787.

138 N. Jaitly, A. Mayampurath, K. Littlefield, J. N. Adkins, G. A. Anderson and R. D. Smith, Decon2LS: an open-source software package for automated processing and visualization of high resolution mass spectrometry data, *BMC Bioinf.*, 2009, **10**, 87.

139 E. Kendrick, Mass scale based on CH_2 = 14.0000 for high-resolution mass spectrometry of organic compounds, *Anal. Chem.*, 1963, **35**(13), 2146–2154.

140 A. Korf, T. Fouquet, R. Schmid, H. Hayen and S. Hagenhoff, Expanding the Kendrick Mass Plot Toolbox in MZmine 2 to Enable Rapid Polymer Characterization in Liquid Chromatography–Mass Spectrometry Data Sets, *Anal. Chem.*, 2020, **92**(1), 628–633.

141 P. J. Roach, J. Laskin and A. Laskin, Higher-Order Mass Defect Analysis for Mass Spectra of Complex Organic Mixtures, *Anal. Chem.*, 2011, **83**(12), 4924–4929.

142 R. A. Friedel and M. Orchi, *Ultraviolet Spectra of Aromatic Compounds*, John Wiley & Sons, Inc., New York, 1952, 52pp.

143 A. C. O. Magalhães, J. C. G. Esteves da Silva and L. Pinto da Silva, Density Functional Theory Calculation of the Absorption Properties of Brown Carbon Chromophores Generated by Catechol Heterogeneous Ozonolysis, *ACS Earth Space Chem.*, 2017, **1**(6), 353–360.

Open Access Article. Published on 02 January 2025. Downloaded on 1/23/2026 11:08:06 PM. This article is licensed under a Creative Commons Attribution-NonCommercial 3.0 Unported Licence.

144 C. Xing, Y. Wan, Q. Wang, S. Kong, X. Huang, X. Ge, M. Xie and H. Yu, Molecular Characterization of Brown Carbon Chromophores in Atmospherically Relevant Samples and Their Gas-Particle Distribution and Diurnal Variation in the Atmosphere, *J. Geophys. Res.: Atmos.*, 2023, **128**(12), e2022JD038142.

145 V. V. Lobodin, A. G. Marshall and C. S. Hsu, Compositional Space Boundaries for Organic Compounds, *Anal. Chem.*, 2012, **84**(7), 3410–3416.

146 K. Siegmann and K. Sattler, Formation mechanism for polycyclic aromatic hydrocarbons in methane flames, *J. Chem. Phys.*, 2000, **112**(2), 698–709.

147 J. Cain, A. Laskin, M. R. Kholghy, M. J. Thomson and H. Wang, Molecular characterization of organic content of soot along the centerline of a coflow diffusion flame, *Phys. Chem. Chem. Phys.*, 2014, **16**(47), 25862–25875.

148 A. Arola, G. Schuster, G. Myhre, S. Kazadzis, S. Dey and S. N. Tripathi, Inferring absorbing organic carbon content from AERONET data, *Atmos. Chem. Phys.*, 2011, **11**(1), 215–225.

149 P. A. Makar, A. Akingunola, J. Chen, B. Pabla, W. Gong, C. Stroud, C. Sioris, K. Anderson, P. Cheung, J. Zhang and J. Milbrandt, Forest-fire aerosol–weather feedbacks over western North America using a high-resolution, online coupled air-quality model, *Atmos. Chem. Phys.*, 2021, **21**(13), 10557–10587.

150 F. Li, X. Zhang and S. Kondragunta, Highly anomalous fire emissions from the 2019–2020 Australian bushfires, *Environ. Res. Commun.*, 2021, **3**(10), 105005.

151 H. B. Singh, B. E. Anderson, W. H. Brune, C. Cai, R. C. Cohen, J. H. Crawford, M. J. Cubison, E. P. Czech, L. Emmons, H. E. Fuelberg, G. Huey, D. J. Jacob, J. L. Jimenez, A. Kaduwela, Y. Kondo, J. Mao, J. R. Olson, G. W. Sachse, S. A. Vay, A. Weinheimer, P. O. Wennberg and A. Wisthaler, Pollution influences on atmospheric composition and chemistry at high northern latitudes: Boreal and California forest fire emissions, *Atmos. Environ.*, 2010, **44**(36), 4553–4564.

152 R. A. Washenfelder, A. R. Attwood, C. A. Brock, H. Guo, L. Xu, R. J. Weber, N. L. Ng, H. M. Allen, B. R. Ayres, K. Baumann, R. C. Cohen, D. C. Draper, K. C. Duffey, E. Edgerton, J. L. Fry, W. W. Hu, J. L. Jimenez, B. B. Palm, P. Romer, E. A. Stone, P. J. Wooldridge and S. S. Brown, Biomass burning dominates brown carbon absorption in the rural southeastern United States, *Geophys. Res. Lett.*, 2015, **42**(2), 653–664.

153 V. Selimovic, R. J. Yokelson, C. Warneke, J. M. Roberts, J. de Gouw, J. Reardon and D. W. T. Griffith, Aerosol optical properties and trace gas emissions by PAX and OP-FTIR for laboratory-simulated western US wildfires during FIREX, *Atmos. Chem. Phys.*, 2018, **18**(4), 2929–2948.

154 X. Li, M. Hu, Y. Wang, N. Xu, H. Fan, T. Zong, Z. Wu, S. Guo, W. Zhu, S. Chen, H. Dong, L. Zeng, X. Yu and X. Tang, Links between the optical properties and chemical compositions of brown carbon chromophores in different environments: contributions and formation of functionalized aromatic compounds, *Sci. Total Environ.*, 2021, **786**, 147418.

155 J. W. Knight, J. E. M. Forsythe, X. Zhang, A. Rafferty, A. J. Orr-Ewing and M. I. Cotterell, Wavelength- and pH-Dependent Optical Properties of Aqueous Aerosol Particles Containing 4-Nitrocatechol, *ACS Earth Space Chem.*, 2024, **8**(11), 2198–2208.

156 L. Yang, R.-J. Huang, J. Shen, T. Wang, Y. Gong, W. Yuan, Y. Liu, H. Huang, Q. You, D. D. Huang and C. Huang, New Insights into the Brown Carbon Chromophores and Formation Pathways for Aqueous Reactions of α-Dicarbonyls with Amines and Ammonium, *Environ. Sci. Technol.*, 2023, **57**(33), 12351–12361.

157 L. Yang, R.-J. Huang, W. Yuan, D. D. Huang and C. Huang, pH-Dependent Aqueous-Phase Brown Carbon Formation: Rate Constants and Implications for Solar Absorption and Atmospheric Photochemistry, *Environ. Sci. Technol.*, 2024, **58**(2), 1236–1243.

158 H. Wang, J. Ding, J. Xu, J. Wen, J. Han, K. Wang, G. Shi, Y. Feng, C. E. Ivey, Y. Wang, A. Nenes, Q. Zhao and A. G. Russell, Aerosols in an arid environment: the role of aerosol water content, particulate acidity, precursors, and relative humidity on secondary inorganic aerosols, *Sci. Total Environ.*, 2019, **646**, 564–572.

159 X. Duan, Y. Yan, L. Peng, K. Xie, D. Hu, R. Li and C. Wang, Role of ammonia in secondary inorganic aerosols formation at an ammonia-rich city in winter in north China: a comparative study among industry, urban, and rural sites, *Environ. Poll.*, 2021, **291**, 118151.

160 R.-J. Huang, J. Duan, Y. Li, Q. Chen, Y. Chen, M. Tang, L. Yang, H. Ni, C. Lin, W. Xu, Y. Liu, C. Chen, Z. Yan, J. Ovadnevaite, D. Ceburnis, U. Dusek, J. Cao, T. Hoffmann and C. D. O'Dowd, Effects of NH_3 and alkaline metals on the formation of particulate sulfate and nitrate in wintertime Beijing, *Sci. Total Environ.*, 2020, **717**, 137190.

161 X. Liu, H. Wang, F. Wang, S. Lv, C. Wu, Y. Zhao, S. Zhang, S. Liu, X. Xu, Y. Lei and G. Wang, Secondary Formation of Atmospheric Brown Carbon in China Haze: Implication for an Enhancing Role of Ammonia, *Environ. Sci. Technol.*, 2023, **57**(30), 11163–11172.

162 N. Bluvshtein, P. Lin, J. M. Flores, L. Segev, Y. Mazar, E. Tas, G. Snider, C. Weagle, S. S. Brown, A. Laskin and Y. Rudich, Broadband optical properties of biomass-burning aerosol and identification of brown carbon chromophores, *J. Geophys. Res.: Atmos.*, 2017, **122**(10), 5441–5456.

163 B. R. T. Simoneit, W. F. Rogge, M. A. Mazurek, L. J. Standley, L. M. Hildemann and G. R. Cass, Lignin pyrolysis products, lignans, and resin acids as specific tracers of plant classes in emissions from biomass combustion, *Environ. Sci. Technol.*, 1993, **27**(12), 2533–2541.

164 J. Yus-Díez, V. Bernardoni, G. Močnik, A. Alastuey, D. Ciniglia, M. Ivančič, X. Querol, N. Perez, C. Reche, M. Rigler, R. Vecchi, S. Valentini and M. Pandolfi, Determination of the multiple-scattering correction factor and its cross-sensitivity to scattering and wavelength dependence for different AE33 Aethalometer filter tapes: a multi-

 This journal is © The Royal Society of Chemistry 2025

Open Access Article. Published on 02 January 2025. Downloaded on 1/23/2026 11:08:06 PM. This article is licensed under a Creative Commons Attribution-NonCommercial 3.0 Unported Licence.

instrumental approach, *Atmos. Meas. Tech.*, 2021, **14**(10), 6335–6355.

165 L. Ferrero, N. Losi, M. Rigler, A. Gregorič, C. Colombi, L. D'Angelo, E. Cuccia, A. M. Cefalì, I. Gini, A. Doldi, S. Cerri, P. Maroni, D. Cipriano, P. Markuszewski and E. Bolzacchini, Determining the Aethalometer multiple scattering enhancement factor C from the filter loading parameter, *Sci. Total Environ.*, 2024, **917**, 170221.

166 V. Bernardoni, L. Ferrero, E. Bolzacchini, A. C. Forello, A. Gregorič, D. Massabò, G. Močnik, P. Prati, M. Rigler, L. Santagostini, F. Soldan, S. Valentini, G. Valli and R. Vecchi, Determination of Aethalometer multiple-scattering enhancement parameters and impact on source apportionment during the winter 2017/18 EMEP/ACTRIS/COLOSSAL campaign in Milan, *Atmos. Meas. Tech.*, 2021, **14**(4), 2919–2940.

167 N. M. Donahue, J. H. Kroll, S. N. Pandis and A. L. Robinson, A two-dimensional volatility basis set – Part 2: diagnostics of organic-aerosol evolution, *Atmos. Chem. Phys.*, 2012, **12**(2), 615–634.

168 H. J. L. Forstner, R. C. Flagan and J. H. Seinfeld, Secondary Organic Aerosol from the Photooxidation of Aromatic Hydrocarbons: Molecular Composition, *Environ. Sci. Technol.*, 1997, **31**(5), 1345–1358.

169 M. S. Jang and R. M. Kamens, Characterization of secondary aerosol from the photooxidation of toluene in the presence of NOx and 1-propene, *Environ. Sci. Technol.*, 2001, **35**(18), 3626–3639.

170 K. Sato, S. Hatakeyama and T. Imamura, Secondary organic aerosol formation during the photooxidation of toluene: NO_x dependence of chemical composition, *J. Phys. Chem. A*, 2007, **111**(39), 9796–9808.

171 Q. F. He, C. L. Li, K. Siemens, A. C. Morales, A. P. S. Hettiyadura, A. Laskin and Y. Rudich, Optical Properties of Secondary Organic Aerosol Produced by Photooxidation of Naphthalene under NOx Condition, *Environ. Sci. Technol.*, 2022, **56**(8), 4816–4827.

172 Y. Ren, Z. Wu, Y. Ji, F. Bi, J. Li, H. Zhang, H. Zhang, H. Li and G. Wang, Non-negligible secondary contribution to brown carbon in autumn and winter: inspiration from particulate nitrated and oxygenated aromatic compounds in urban Beijing, *Atmos. Chem. Phys.*, 2024, **24**(11), 6525–6538.

173 K. Sato, A. Takami, Y. Kato, T. Seta, Y. Fujitani, T. Hikida, A. Shimono and T. Imamura, AMS and LC/MS analyses of SOA from the photooxidation of benzene and 1,3,5-trimethylbenzene in the presence of NO_x: effects of chemical structure on SOA aging, *Atmos. Chem. Phys.*, 2012, **12**(10), 4667–4682.

174 B. Ervens, B. J. Turpin and R. J. Weber, Secondary organic aerosol formation in cloud droplets and aqueous particles (aqSOA): a review of laboratory, field and model studies, *Atmos. Chem. Phys.*, 2011, **11**(21), 11069–11102.

175 Z. N. Xu, W. Nie, Y. L. Liu, P. Sun, D. D. Huang, C. Yan, J. Krechmer, P. L. Ye, Z. Xu, X. M. Qi, C. J. Zhu, Y. Y. Li, T. Y. Wang, L. Wang, X. Huang, R. Z. Tang, S. Guo, G. L. Xiu, Q. Y. Fu, D. Worsnop, X. G. Chi and A. J. Ding, Multifunctional Products of Isoprene Oxidation in Polluted Atmosphere and Their Contribution to SOA, *Geophys. Res. Lett.*, 2021, **48**(1), e2020GL089276.

176 Y. H. Lin, H. Budisulistiorini, K. Chu, R. A. Siejack, H. F. Zhang, M. Riva, Z. F. Zhang, A. Gold, K. E. Kautzman and J. D. Surratt, Light-Absorbing Oligomer Formation in Secondary Organic Aerosol from Reactive Uptake of Isoprene Epoxydiols, *Environ. Sci. Technol.*, 2014, **48**(20), 12012–12021.

177 A. A. O. Sarhan and C. Bolm, Iron(III) chloride in oxidative C–C coupling reactions, *Chem. Soc. Rev.*, 2009, **38**(9), 2730–2744.

178 D. O. De Haan, E. Tapavicza, M. Riva, T. Cui, J. D. Surratt, A. C. Smith, M.-C. Jordan, S. Nilakantan, M. Almodovar, T. N. Stewart, A. de Loera, A. C. De Haan, M. Cazaunau, A. Gratien, E. Pangui and J.-F. Doussin, Nitrogen-Containing, Light-Absorbing Oligomers Produced in Aerosol Particles Exposed to Methylglyoxal, Photolysis, and Cloud Cycling, *Environ. Sci. Technol.*, 2018, **52**(7), 4061–4071.

179 A. A. Rodriguez, M. A. Rafla, H. G. Welsh, E. A. Pennington, J. R. Casar, L. N. Hawkins, N. G. Jimenez, A. de Loera, D. R. Stewart, A. Rojas, M. K. Tran, P. Lin, A. Laskin, P. Formenti, M. Cazaunau, E. Pangui, J. F. Doussin and D. O. De Haan, Kinetics, Products, and Brown Carbon Formation by Aqueous-Phase Reactions of Glycolaldehyde with Atmospheric Amines and Ammonium Sulfate, *J. Phys. Chem. A*, 2022, **126**(32), 5375–5385.

180 N. G. Jimenez, K. D. Sharp, T. Gramyk, D. Z. Ugland, M.-K. Tran, A. Rojas, M. A. Rafla, D. Stewart, M. M. Galloway, P. Lin, A. Laskin, M. Cazaunau, E. Pangui, J.-F. Doussin and D. O. De Haan, Radical-Initiated Brown Carbon Formation in Sunlit Carbonyl–Amine–Ammonium Sulfate Mixtures and Aqueous Aerosol Particles, *ACS Earth Space Chem.*, 2022, **6**(1), 228–238.

181 P. K. Aiona, H. J. Lee, R. Leslie, P. Lin, A. Laskin, J. Laskin and S. A. Nizkorodov, Photochemistry of Products of the Aqueous Reaction of Methylglyoxal with Ammonium Sulfate, *ACS Earth Space Chem.*, 2017, **1**(8), 522–532.

182 P. K. Aiona, H. J. Lee, P. Lin, F. Heller, A. Laskin, J. Laskin and S. A. Nizkorodov, A Role for 2-Methyl Pyrrole in the Browning of 4-Oxopentanal and Limonene Secondary Organic Aerosol, *Environ. Sci. Technol.*, 2017, **51**(19), 11048–11056.

183 D. L. Bones, D. K. Henricksen, S. A. Mang, M. Gonsior, A. P. Bateman, T. B. Nguyen, W. J. Cooper and S. A. Nizkorodov, Appearance of strong absorbers and fluorophores in limonene-O3 secondary organic aerosol due to NH4+-mediated chemical aging over long time scales, *J. Geophys. Res.: Atmos.*, 2010, **115**(D5), D05203, DOI: **10.1029/2009JD012864**.

184 J. Laskin, A. Laskin, S. A. Nizkorodov, P. Roach, P. Eckert, M. K. Gilles, B. Wang, H. J. Lee and Q. Hu, Molecular Selectivity of Brown Carbon Chromophores, *Environ. Sci. Technol.*, 2014, **48**(20), 12047–12055.

185 J. Laskin, A. Laskin, P. J. Roach, G. W. Slysz, G. A. Anderson, S. A. Nizkorodov, D. L. Bones and L. Q. Nguyen,

Open Access Article. Published on 02 January 2025. Downloaded on 1/23/2026 11:08:06 PM. This article is licensed under a Creative Commons Attribution-NonCommercial 3.0 Unported Licence.

High-Resolution Desorption Electrospray Ionization Mass Spectrometry for Chemical Characterization of Organic Aerosols, *Anal. Chem.*, 2010, **82**(5), 2048–2058.

186 J. Montoya-Aguilera, J. R. Horne, M. L. Hinks, L. T. Fleming, V. Perraud, P. Lin, A. Laskin, J. Laskin, D. Dabdub and S. A. Nizkorodov, Secondary organic aerosol from atmospheric photooxidation of indole, *Atmos. Chem. Phys.*, 2017, **17**(18), 11605–11621.

187 H. Chin, K. S. Hopstock, L. T. Fleming, S. A. Nizkorodov and H. A. Al-Abadleh, Effect of aromatic ring substituents on the ability of catechol to produce brown carbon in iron(III)–catalyzed reactions, *Environ. Sci.: Atmos.*, 2021, **1**(2), 64–78.

188 K. S. Hopstock, B. P. Carpenter, J. P. Patterson, H. A. Al-Abadleh and S. A. Nizkorodov, Formation of insoluble brown carbon through iron-catalyzed reaction of biomass burning organics, *Environ. Sci.: Atmos.*, 2023, **3**(1), 207–220.

189 H. A. Al-Abadleh, M. S. Rana, W. Mohammed and M. I. Guzman, Dark Iron-Catalyzed Reactions in Acidic and Viscous Aerosol Systems Efficiently Form Secondary Brown Carbon, *Environ. Sci. Technol.*, 2021, **55**(1), 209–219.

190 F. K. A. Gregson, N. G. A. Gerrebos, M. Schervish, S. Nikkho, E. G. Schnitzler, C. Schwartz, C. Carlsten, J. P. D. Abbatt, S. Kamal, M. Shiraiwa and A. K. Bertram, Phase Behavior and Viscosity in Biomass Burning Organic Aerosol and Climatic Impacts, *Environ. Sci. Technol.*, 2023, **57**(39), 14548–14557.

191 C. Liu-Kang, P. J. Gallimore, T. Y. Liu and J. P. D. Abbatt, Photoreaction of biomass burning brown carbon aerosol particles, *Environ. Sci.: Atmos.*, 2022, **2**(2), 270–278.

192 R. Zhao, A. K. Y. Lee, L. Huang, X. Li, F. Yang and J. P. D. Abbatt, Photochemical processing of aqueous atmospheric brown carbon, *Atmos. Chem. Phys.*, 2015, **15**(11), 6087–6100.

193 B. J. Sumlin, A. Pandey, M. J. Walker, R. S. Pattison, B. J. Williams and R. K. Chakrabarty, Atmospheric Photooxidation Diminishes Light Absorption by Primary Brown Carbon Aerosol from Biomass Burning, *Environ. Sci. Technol. Lett.*, 2017, **4**(12), 540–545.

194 C. L. Li, Q. F. He, J. Schade, J. Passig, R. Zimmermann, D. Meidan, A. Laskin and Y. Rudich, Dynamic changes in optical and chemical properties of tar ball aerosols by atmospheric photochemical aging, *Atmos. Chem. Phys.*, 2019, **19**(1), 139–163.

195 J. P. S. Wong, M. Tsagkaraki, I. Tsiodra, N. Mihalopoulos, K. Violaki, M. Kanakidou, J. Sciare, A. Nenes and R. J. Weber, Atmospheric evolution of molecular-weight-separated brown carbon from biomass burning, *Atmos. Chem. Phys.*, 2019, **19**(11), 7319–7334.

196 Z. Cheng, K. M. Atwi, Z. Yu, A. Avery, E. C. Fortner, L. Williams, F. Majluf, J. E. Krechmer, A. T. Lambe and R. Saleh, Evolution of the light-absorption properties of combustion brown carbon aerosols following reaction with nitrate radicals, *Aerosol Sci. Technol.*, 2020, **54**(7), 849–863.

197 A. B. Dalton and S. A. Nizkorodov, Photochemical Degradation of 4-Nitrocatechol and 2,4-Dinitrophenol in a Sugar-Glass Secondary Organic Aerosol Surrogate, *Environ. Sci. Technol.*, 2021, **55**(21), 14586–14594.

198 E. G. Schnitzler, N. G. A. Gerrebos, T. S. Carter, Y. Huang, C. L. Healdc, A. K. Bertram and J. P. D. Abbatt, Rate of atmospheric brown carbon whitening governed by environmental conditions, *Proc. Natl. Acad. Sci. U. S. A.*, 2022, **119**(38), e2205610119.

199 J. Y. Chen, E. Rodriguez, H. H. Jiang, K. P. Chen, A. Frie, H. F. Zhang, R. Bahreini and Y. H. Lin, Time-Dependent Density Functional Theory Investigation of the UV-Vis Spectra of Organonitrogen Chromophores in Brown Carbon, *ACS Earth Space Chem.*, 2020, **4**(2), 311–320.

200 Q. F. He, S. Tomaz, C. L. Li, M. Zhu, D. Meidan, M. Riva, A. Laskin, S. S. Brown, C. George, X. M. Wang and Y. Rudich, Optical Properties of Secondary Organic Aerosol Produced by Nitrate Radical Oxidation of Biogenic Volatile Organic Compounds, *Environ. Sci. Technol.*, 2021, **55**(5), 2878–2889.

201 H. H. Jiang, A. L. Frie, A. Lavi, J. Y. Chen, H. F. Zhang, R. Bahreini and Y. H. Lin, Brown Carbon Formation from Nighttime Chemistry of Unsaturated Heterocyclic Volatile Organic Compounds, *Environ. Sci. Technol. Lett.*, 2019, **6**(3), 184–190.

202 K. McNeill and S. Canonica, Triplet state dissolved organic matter in aquatic photochemistry: reaction mechanisms, substrate scope, and photophysical properties, *Environ. Sci.: Processes Impacts*, 2016, **18**(11), 1381–1399.

203 R. Kaur and C. Anastasio, First Measurements of Organic Triplet Excited States in Atmospheric Waters, *Environ. Sci. Technol.*, 2018, **52**(9), 5218–5226.

204 L. Yu, J. Smith, A. Laskin, C. Anastasio, J. Laskin and Q. Zhang, Chemical characterization of SOA formed from aqueous-phase reactions of phenols with the triplet excited state of carbonyl and hydroxyl radical, *Atmos. Chem. Phys.*, 2014, **14**(24), 13801–13816.

205 L. Yu, J. Smith, A. Laskin, K. M. George, C. Anastasio, J. Laskin, A. M. Dillner and Q. Zhang, Molecular transformations of phenolic SOA during photochemical aging in the aqueous phase: competition among oligomerization, functionalization, and fragmentation, *Atmos. Chem. Phys.*, 2016, **16**(7), 4511–4527.

206 R. Kaur, B. Hudson, J. Draper, D. Tantillo and C. Anastasio, Aqueous reactions of organic triplet excited states with atmospheric alkenes, *Atmos. Chem. Phys.*, 2019, **19**, 5021–5032.

207 R. G. Zepp, P. F. Schlotzhauer and R. M. Sink, Photosensitized transformations involving electronic energy transfer in natural waters: role of humic substances, *Environ. Sci. Technol.*, 1985, **19**(1), 74–81.

208 C. Anastasio, B. C. Faust and C. J. Rao, Aromatic Carbonyl Compounds as Aqueous-Phase Photochemical Sources of Hydrogen Peroxide in Acidic Sulfate Aerosols, Fogs, and Clouds. 1. Non-Phenolic Methoxybenzaldehydes and Methoxyacetophenones with Reductants (Phenols), *Environ. Sci. Technol.*, 1997, **31**(1), 218–232.

 This journal is © The Royal Society of Chemistry 2025